Deciphering the impact of fructose metabolism on liver mitochondrial bioenergetics

By
Katherine A. Buddo
December 2021

Director of Dissertation: P. Darrell Neufer

Department of Physiology

Since its discovery in 1980, the interest in nonalcoholic fatty liver disease, the liver manifestation of metabolic syndrome, has expanded due to the growing impact on the world's health. Commonly characterized by ≥5% hepatic lipid accumulation in the absence of a secondary cause, NAFLD is a broad term used to encompass a variety of disease states within the liver. The largest predictor of NAFLD is said to metabolic syndrome itself, with type 2 diabetes being the most prevalent link. Currently, up to 75% of diabetic individuals also have a NAFLD diagnosis. It is also known that individuals diagnosed with NAFLD exhibit lower mitochondrial function overall. While the mechanism is largely unknown, fructose consumption has been specifically linked to the development and progression of NAFLD.

Fructose metabolism differs from that of glucose metabolism. Unlike glucose, fructose has been shown to increase glucose, glycogen, lactate, uric acid, and pyruvate as end products, as well as a small increase in diet-induced thermogenesis. One major difference in metabolism is the production of uric acid following fructose metabolism. As fructose is brought into the liver, it is rapidly phosphorylated to fructose-1-phospate. This rapid use of ATP increases the generation of AMP and subsequent flux through the purine degradation pathway, ultimately leading to an increase in uric acid production in the liver. A second finding of note is that this phosphorylation

process leads to an immediate drop in available ATP within the liver. Since it is unlikely that the cell's ATP usage outpaces its ability to resynthesize ATP using oxidative phosphorylation, there is a possibility that fructose metabolism leads to a decline in mitochondrial function, the primary site of ATP production. Overall, this project set out to determine if the metabolism of fructose, and subsequent production of uric acid, was the driving factor behind the decline of mitochondrial function in the liver.

In Aim 1 of this project, the impact of fructose was directly determined. This was done by gavaging mice with both fructose and glucose to determine the mitochondrial changes associated with each sugar source. It was determined that an acute gavage of both glucose and fructose lead to increases in uric acid production in the liver, accompanied by increases in the oxygen consumption rates of the mitochondria isolated from these mice. It was also found that the measured differences between treatment groups was a transient measurement, in which there was only a difference 15-minutes post gavage, and by 60-minutes, there was no impact on mitochondrial function. Additionally, when treated over a 14-day period, there were no changes in mitochondrial function. This aim found that overall there were increase in oxygen consumption rates associated with increases in uric acid production.

To better determine the potential direct impact of uric acid on mitochondrial function, Aim 2 was designed. It was found that the addition of uric acid to the system elicited a dose dependent increase in oxygen consumption rate. Using this dose dependent response, an optimal concentration was determined to carry out the remaining assays. From this aim, it was determined that there was an increase in oxygen consumption rate following the addition of uric acid. This increase was found to be present both in the presence and absence of adenylates. When each complex was examined individually, it was determined that there was no single

mitochondrial source linked to the increase in oxygen consumption rate. Rodents retain urate oxidase, whereas humans do not. The known inhibitor of urate oxidase, potassium oxonate, was used to determine if urate oxidase was in fact the source of residual oxygen consumption rate. Once added, it was determined that potassium oxonate was sufficient to inhibit the residual oxygen consumption. Additionally, the presence of potassium oxonate did not impact mitochondrial function alone.

Overall, this project set out to determine the impact of fructose and uric acid on mitochondrial function. It was thought that both fructose and uric acid would lead to a decline in the mitochondrial function, resulting in an inability to produce, and therefore maintain, the ATP concentration. This was not what was found. It was determined that neither fructose nor uric acid was sufficient to lead to a decline in mitochondrial bioenergetic function. Instead, it was found that all oxygen consumption observations were due to the presence of urate oxidase and its consumption of oxygen during the metabolization of uric acid. This is a novel finding in that it does not agree with the current literature, which suggests both fructose and uric acid lead to mitochondrial decline.

Deciphering the impact of fructose metabolism on liver mitochondrial bioenergetics

A Dissertation
Presented to the Faculty of the Department of Physiology
Brody School of Medicine
East Carolina University

In Partial Fulfillment of the Requirements for the Degree
Doctor of Philosophy in Biomedical Sciences

By
Katherine A. Buddo
December 2021

Determining the impact of fructose metabolism on liver mitochondrial bioenergetics

By
Katherine A. Buddo

APPROVED BY:

DISSERTATION ADVISOR: _____
P. Darrell Neufer, PhD

COMMITTEE MEMBER:
_____
Kelsey H. Fisher-Wellman, PhD

COMMITTEE MEMBER:
_____
Johanna L. Hannan, PhD

COMMITTEE MEMBER:
_____
Tonya N. Zeczycki, PhD

CHAIR OF THE DEPARTMENT OF PHYSIOLOGY:

_____
Robert Lust, PhD

DEAN OF THE GRADUATE SCHOOL:

_____
Paul J. Gemperline, PhD

TABLE OF CONTENTS

LIST OF FIGURES

LIST OF SYMBOLS AND ABBREVIATIONS

$\Delta G'_{ATP}$ – Change in ATP Free Energy

AldoB – Aldolase B

ADP – Adenosine Diphosphate

AMP – Adenosine Monophosphate

AntiA – Antimycin A

AP5A - P1,P5-di(adenosine-5′) pentaphosphate

Asc - Ascorbate

ATP – Adenosine Triphosphate

Carn – Carnitine

CoA – Coenzyme A

DHAP – dihydroxyacetone phosphate

ETS – Electron Transport System

FCCP - Trifluoromethoxy carbonylcyanide phenylhydrazone

F1P – Fructose-1-Phosphate

G6P – Glucose-6-phosphate

Glu – Glutamate

Glut-2 – Glucose Transporter (2)

Glut 5- Glucose Transporter (5)

HCC – Hepatocellular Carcinoma

HFCS – High Fructose Corn Syrup

*J*ATP – Rate of ATP Production

JO_2 – Rate of Respiration

KHK – Ketohexokinase

KOX – Potassium Oxonate

Mal – Malate

Malo – Malonate

$NADH/NAD^{+}$ - Reduced/Oxidized Nicotinamide Adenine Dinucleotide

$NADPH/NADP^{+}$ - Reduced/Oxidized Nicotinamide Adenine Dinucleotide Phosphate

NAFL – Non-alcoholic Fatty Liver

NAFLD – Non-alcoholic Fatty Liver Disease

NASH – Non-alcoholic Steatohepatitis

O2K – Oroboros Instruments Oxygraph-2K

Oct – Octanoyl-Carnitine

Oligo - Oligomycin

OXPHOS – Oxidative Phosphorylation

PC – Palmitoyl-Carnitine

PCoA – Palmitoyl-CoA

PFK - Phosphofructokinase

Pyr – Pyruvate

Rot - Rotenone

Succ - Succinate

TCA – Tricarboxylic Acid

TG – Triglyceride

TMRM - Tetramethylrhodamine, methyl ester

TMPD - N, N, N′, N′-tetramethyl- p -phenylenediamine

VLDL – Very Low-Density Lipoprotein

Chapter 1: Introduction

Nonalcoholic Fatty Liver Disease:

Worldwide, the prevalence of type 2 diabetes, obesity, and metabolic syndrome is said to be epidemic[1–3]. First discovered in 1980, nonalcoholic fatty liver disease (NAFLD) is understood to be the manifestation of metabolic syndrome in the liver[1,4,5]. In recent years, interest in NAFLD disease and its progression has expanded due to the growing impact on the world's health[6]. As of 2015 approximately 83.1 million individuals had been diagnosed with NAFLD in the United States alone[6]. That number is expected to reach around 100.9 million by 2030[6]. As patients progress through the disease, there is an increased incidence of cirrhosis, end-stage liver disease which requires a transplant, and hepatocellular carcinoma[4,6]. These physical manifestations naturally result in an increased economic burden, not to mention an increased risk of mortality if left untreated[4].

NAFLD is characterized by ≥5% hepatic lipid accumulation in the absence of a secondary cause. Therefore, the diagnosis is commonly one of exclusion. Currently, NAFLD is a broad term used to describe a multitude of symptoms and disease states within the liver. Nonalcoholic fatty liver (NAFL), nonalcoholic steatohepatitis (NASH), fibrosis, NASH cirrhosis, NASH-related hepatocellular carcinoma (HCC) all fall within the NAFLD classification[4]. Generally, a liver biopsy is used to diagnose NAFLD; however, a hepatic ultrasonogram, computed tomography (CT) scan, blood test, liver enzyme test, or MRI are also commonly accepted diagnostic techniques[4]. Due to the varying availability of technologies used to diagnose NAFLD, reporting

rates vary globally. Differences in dietary habits and physical activity levels also play a role in the regional differences of reported cases[4].

In general, a healthy liver consists of 5.5% fat or less, meaning a healthy liver is not storing substantial amounts of fat. Fatty livers are generally caused by an imbalance among the import, synthesis, utilization, and export of fat. In NAFLD, fatty acid synthesis has been identified as a source of dysregulation within the system. In individuals with NAFLD, fatty acid synthesis (i.e., *de novo* lipogenesis) has be found to be elevated by as much as 5-fold [7], very low-density lipoprotein (VLDL)[8,9] and triglyceride (TG)[10] secretion is increased, and the clearance of TG is delayed[11]. Overall, this dysregulation of synthesis, secretion, and subsequent clearance underlies the accumulation of TG deposits within the liver[12].

Metabolic syndrome, defined as obesity, hyperglycemia, dyslipidemia, and systematic hypertension, is currently the largest predictor of NAFLD. The relationship is said to be bidirectional, meaning not only does metabolic syndrome increase the risk of NAFLD, but NAFLD may exacerbate some metabolic syndrome ailments[6]. As of now, type 2 diabetes is the most prevalent link to NAFLD, with up to 75% of diabetic individuals also having a NAFLD diagnosis[6]. In recent years, the consumption of fructose and fructose sweetened beverages specifically has been linked to the development and progression of NAFLD[12–19].

Fructose in the development of NAFLD:

Fructose can be found in a monosaccharide form or a disaccharide form in which it is bound to glucose to form sucrose. The primary dietary forms of fructose are high fructose corn syrup (HFCS) and sucrose (cane sugar). While the United States is the major user of HFCS, it is produced and used worldwide[20]. HFCS was first introduced to the consumer market in 1967, and by 1990, fructose intake had increased by 50%[12,20].

Fructose vs. Glucose:

Fructose metabolism and absorption differs from that of glucose. It is absorbed in the duodenum and jejunum. After absorption, both glucose and fructose enter the portal circulation and are transported to the liver. Here fructose can be converted into glucose and used for further processes. When consumed in small amounts, fructose increases glycogen synthesis and reduces glycemic response in diabetic (type 2) human subjects[20]. However, when given in large quantities, fructose provides an unregulated source of intermediates for hepatic lipogenesis[20]. It has also been shown that fructose intake produces an increase in glucose, glycogen, lactate, uric acid, and pyruvate as end products[21], as well as a small increase in diet-induced thermogenesis[22]. This indicates that the metabolic fates, and subsequent effects, of glucose and fructose are different[22].

In addition to absorption locations, glucose and fructose metabolism differ in transporters. Glucose is transported into the liver using GLUT-2 then phosphorylated by Glucokinase to become glucose-6-phosphate (G6P). Phosphofructokinase (PFK) can then use G6P and convert it to the

glycerol backbone of triacylglycerols. However, fructose is transported into the cell by GLUT-5, which is non-insulin dependent[23]. Interestingly, GLUT-5 transporters are not expressed in either pancreatic ß-cells or the brain[21,23], partially explaining why fructose, in contrast with glucose, does not elicit the release of insulin from β-cells or a sensation of "satiety" in the appetite control center of the brain[21].

Fructose metabolism:

Fructose is rapidly taken up from the portal circulation and metabolized almost exclusively by the liver[24]. **Figure 1** shows the fructose metabolism pathway inside a cell. Once in the cell, fructose is rapidly phosphorylated by Ketohexokinase (KHK) into fructose-1-phosphate (F1P), which is an ATP dependent process[23]. Following phosphorylation, F1P is cleaved by Aldolase B (AldoB) to form glyceraldehyde and dihydroxyacetone phosphate (DHAP) and then later into intermediates that feed into multiple pathways including triglyceride synthesis, gluconeogenesis, and glycolysis. Glucose metabolism in the liver is a regulated process due in part to feedback regulation imposed on Glucokinase any time the reaction product, G6P, builds up. In contrast, fructose metabolism is not regulated in the liver, due in part to the absence of feedback inhibition on Ketohexokinase by F1P. Also, unlike glucose metabolism, F1P is cleaved by Aldolase B, bypassing the PFK reaction which is subject to multiple levels of allosteric regulation. The products of fructose metabolism feed directly into the fatty acid synthesis pathways. The net result is the uptake, phosphorylation, and catabolism of fructose is determined by the amount of dietary fructose intake alone.

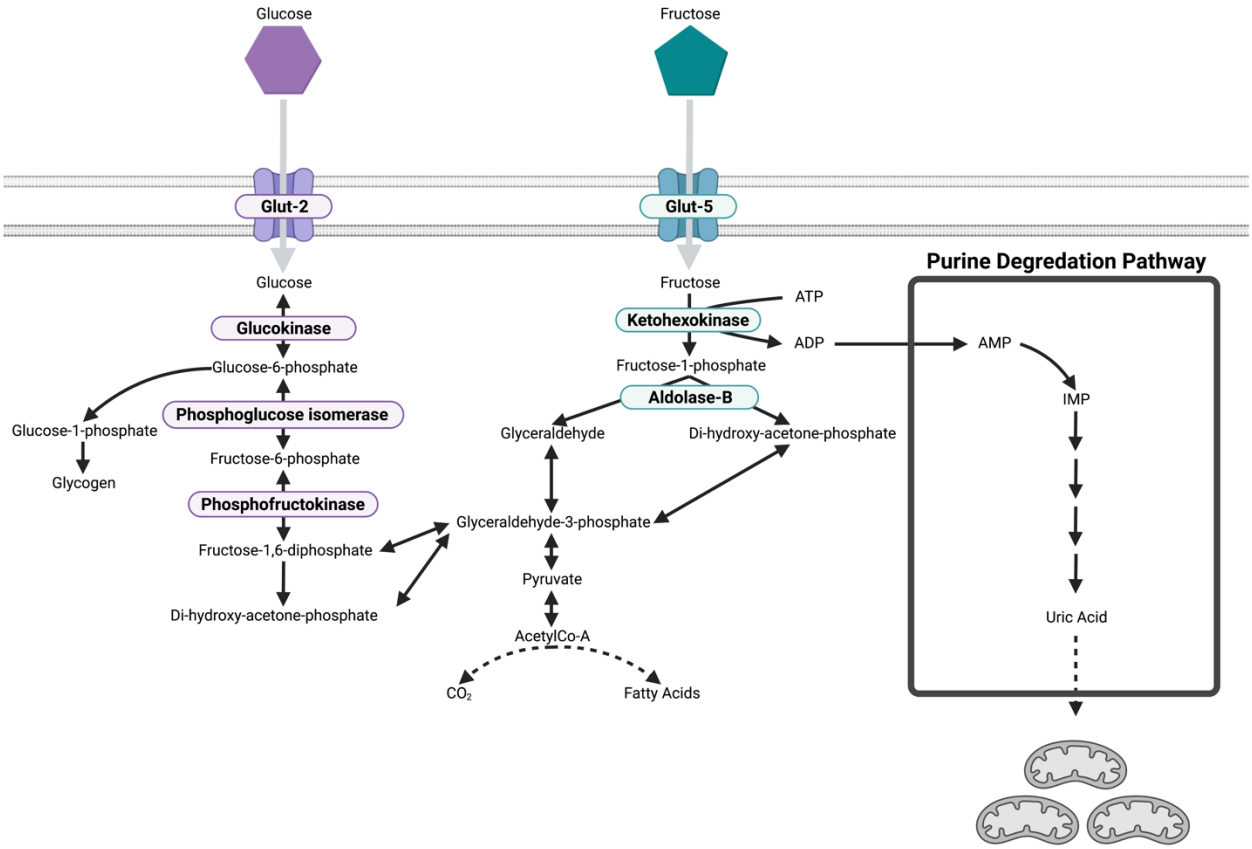

Figure 1: Fructose metabolism pathway including the connection to the purine degradation pathway.

Fructose metabolism and ATP depletion:

One striking observation is that fructose feeding induces a rapid decline in ATP levels in both human and rodent models[25–28]. For example, Hultman et al. found that ATP levels drop from 9.03 mmol/kg to 6.15 mmol/kg within 70 minutes of a fructose infusion[26]. All cells typically respond to any increase in ATP utilization by activating a matching rate of ATP re-synthesis via oxidative phosphorylation (OXPHOS) and glycolysis. So, it seems unlikely that the rate of ATP utilization from fructose is so high that it outpaces ATP re-synthesis via glycolysis and OXPHOS. Moreover, the liver is able to meet the demand for ATP in numerous other energy demanding

processes (i.e., gluconeogenesis, etc.) without difficulty. The other possibility that could account for such a rapid fall in ATP is that the uptake and subsequent metabolism of fructose itself could directly or indirectly interfere with mitochondrial OXPHOS, the primary site of ATP production. Previous labs have found evidence that suggest fructose intake alone leads to mitochondrial dysfunction marked by decreased mitochondrial size and protein mass, marked by a decrease in abundance, within the mitochondria themselves[29].

Fructose metabolism and uric acid production:

A second feature unique to fructose catabolism is the production of uric acid[30–32]. As stated before, during fructose catabolism, there is a significant decline in the cellular ATP levels[33–35]. This is coupled with an increase in the degradation of AMP to uric acid[25–27]. While the underlying mechanism behind the rapid mismatch between rates of ATP utilization and ATP production upon fructose intake remains unknown, the consequence of this mismatch is illustrated in mice lacking Aldolase B (AldoB)[36–38]. Mice lacking Aldolase B have significantly lower ATP levels and a significant rise in plasma uric acid levels in response to fructose intake[36–38]. It is also of note that in mice lacking Aldolase B, there is a 100% fatality rate within 72-hours of high fructose intake[36–38]. However, when the same mice lacking AldoB are treated with allopurinol, a xanthine oxidase inhibitor, there is a 100% survival rate after fructose exposure[36,37,39].

It has also been suggested that uric acid generation resulting from purine degradation is responsible for triggering the increase in lipid synthesis in the liver cells[15,40,41]. Uric acid has also been linked to the activation of NADPH oxidase translocase[40], reduction of fatty acid oxidation[1,29],

and an increase in overall mitochondrial oxidative stress[42]. This leads to the theory that uric acid is the mediating factor in the decline of mitochondrial bioenergetic function.

Central Hypothesis:

Fructose intake and metabolism have been linked to the decline of mitochondrial bioenergetics, ultimately leading to the development and progression of obesity and obesity related diseases such as type 2 diabetes, metabolic syndrome, and nonalcoholic fatty liver disease (NAFLD)[15,21,29,43,44]. While it has been shown that fructose intake and metabolism are directly linked to decreased ATP availability[25,26,45] as well as increased uric acid production[13,26,28], it is unclear which factor of the pathway, fructose vs uric acid, is the driving force behind the observed mitochondrial decline. The work of this dissertation was designed to explore two main aims: 1) To determine the impact of fructose administration on liver mitochondrial bioenergetics, and 2) To determine the direct impact of uric acid on liver mitochondrial bioenergetics. The central hypothesis was that fructose ingestion and metabolism induces a dose-dependent and progressive fructose to AMP to uric acid induced mitochondrial bioenergetic failure. Consequently, it was hypothesized that all alterations to mitochondria bioenergetics following a fructose feeding may stem from the production and presence of uric acid in the system. The following data set out to answer this question. This began in Chapter 2 by determining the impact that fructose exposure had on liver mitochondria. Since uric acid is a final product of fructose metabolism, Chapter 3 set out to determine the direct impact of uric acid, the ultimate end product, on mitochondrial function. Chapter 4 then brought the findings together to help give insight to the overall mechanism behind the proposed decline of mitochondrial function in the liver because of fructose exposure. By

understanding the role fructose, and subsequently uric acid, plays in the decline of mitochondrial bioenergetic, therapeutics can potentially be developed to help alleviate the impact.

CHAPTER 2: Impact of direct fructose exposure, both acute and chronic, on mitochondrial bioenergetics in liver mitochondria

INTRODUCTION:

Previous studies have suggested that fructose, as opposed to glucose, is the main driving factor behind the increased prevalence of obesity related disease in the Western world[21,43]. Since 1970, fructose consumption has increased steadily due to the increased usage if high fructose corn syrup in processed foods[21]. The increase in intake of these foods has been correlated to an increase in the development of obesity and obesity related diseases, such as type 2 diabetes and nonalcoholic fatty liver disease[29].

Fructose, once absorbed, is transported to the liver via the portal vein, where it is metabolized. Once in the liver, fructose is phosphorylated by ketohexokinase, generating fructose-1-phosphate (F1P). Unlike glucose metabolism in which further glucose uptake is inhibited by the presence of the glucokinase product, glucose-6-phospate, F1P does not inhibit fructose uptake and subsequent phosphorylation. Due to the unregulated phosphorylation of fructose by ketohexokinase, there is an observed drop in ATP levels within the hepatocyte following a fructose load, yet the direct mechanism for this drop in ATP is not fully understood. F1P is then cleaved by Aldolase B to give glyceraldehyde and dihydroxyacetone phosphate, both of which can be further processed into glyceraldehyde-3-phosphate. Ultimately, this process bypasses phosphofructokinase, which is the rate limiting step in glycolysis, resulting in large increases in glucose, glycogen, lactate, uric acid, and pyruvate as end products[21].

In mice, it has been suggested that fructose exposure and subsequent metabolism is responsible for mitochondrial decline in hepatocytes, ultimately leading to an increased risk for the development and progression of obesity and obesity related diseases[1,21,31]. While mitochondria have been the focus of previous studies, an in-depth interrogation of function itself has not been done. This study aimed to determine the direct impact of both fructose and glucose on liver mitochondrial function in a mouse model.

RESEARCH DESIGN AND METHODS

Buffers:

Buffer A: 50mM MOPS buffer supplemented with 100mM KCl, 1mM EGTA, and 5mM $MgSO_4$, pH 7.1, stored at 4°C.

Buffer B: 50mM MOPS buffer supplemented with 100mM KCl, 1mM EGTA, 5mM $MgSO_4$, and 0.2% BSA, pH 7.1, stored at 4°C.

Buffer C: 105mM MES Potassium salt supplemented with 30mM KCl, 1mM EGTA, 10mM Potassium Phosphate (monobasic), 5mM Magnesium Chloride, 0.25% BSA, pH 7.2, stored at 4°C.

Buffer D: 105mM MES Potassium salt supplemented with 30mM KCl, 1mM EGTA, 10mM Potassium Phosphate (monobasic), 5mM Magnesium Chloride, 0.25% BSA, and 5mM Creatine monohydrate, pH 7.2, stored at 4°C.

Chemicals:

Unless otherwise stated, all chemicals were purchased from Sigma-Aldrich.

Animals:

All animal studies were approved by the East Carolina University Institutional Animal Care and Use Committee. C57BL/6NJ male mice were purchased from Jackson Laboratory. All mice were housed in a temperature (22°C) and light controlled (12-hour light/12-hour dark) room and given free access to food and water. All young mice were 8-weeks old, while the mature mice were 16-weeks old. Unless otherwise stated, mice were anesthetized with isoflurane before tissue removal.

Gavage:

All animals were fasted for 6 hours prior to final gavage. Acutely treated mice were given a single gavage of either 20% fructose or 20% glucose at a dose of 2g/kg/BW[46–49]. Control mice were gavaged with water. Chronically treated mice were gavaged daily for 14-consecutive days at the before mentioned dose. Prior to tissue harvest, mice were fasted for 6-hours[37] and gavaged a final time. The time points for harvest were set at 15-minutes, 30-minutes, and 60-minutes post gavage[25,26,31].

Uric Acid Quantification:

Blood Sample:

Blood was collected at 15-minutes and 60-minutes post gavage and spun down at room temperature for 10 minutes at 2.0 X G. The supernatant with resulting plasma was collected and tested[48].

Liver Sample:

Fresh liver tissue was collected and used for uric acid quantification. The liver section was transferred to a borosilicate glass vessel and homogenized for ~10 passes using a Teflon pestle.

The homogenate was then spun at 800 X G for 10 minutes at 4°C. Following this spin, an aliquot of the homogenate was transferred to the plate.

Both samples were then transferred to a plate. An aliquot of Buffer E was then added to each sample and immediately placed in the plate reader. The plate was read at an Excitation/Emission of 520-590nm at 37°C. A uric acid standard curve was run each day along with samples in duplicate. Standard curve also included a control sample. This assay utilized the uric acid to allantoin reaction using uricase as the catalyst. Amplex UltraRed was coupled with H2O2 and used as the signal readout[32,50,51].

Mitochondrial Isolation:

Once tissue was removed, it was placed in approximately 15mL ice-cold Buffer B. The tissue was then homogenized for approximately 10 passes using a Teflon pestle and borosilicate glass vessel. The homogenized solution was then transferred to a 50mL Falcon tube, and the volume was brought to approximately 30mL. The homogenate was then spun at 800 x G for 10 minutes at 4°C. The subsequent supernatant was then poured through two layers of gauze into a second 50mL Falcon tube, and the volume was then adjusted to approximately 40mL using Buffer A. The solution was then spun again at 10,000 x G for 10 minutes at 4°C. Following the spin, the supernatant was discarded, and the subsequent pellet was washed with 1.4mL of ice-cold Buffer A. The solution was transferred into a 1.7mL tube before being spun again at 10,000 x G for 10 minutes at 4°C. Following this spin, the supernatant was again discarded, and the final pellet was resuspended in 1mL ice-cold Buffer A. A Pierce BCA assay was then performed on the final

solution to determine protein content. Functional assays involving the isolated mitochondria were then carried out in Buffer D [52–54].

Respiration Assays:

Unless otherwise stated, all mitochondrial respiration assays were carried out in Buffer D.

Mitochondrial Respiratory Control:

All mitochondrial respiration measurements were made using a high resolution Oxygraph-2K (Oroboros Instruments) at 37°C. To measure the respiratory control of the mitochondria, a modified version of the creatine kinase clamp assay was utilized [55,56]. This assay utilizes steady-state oxygen consumption rates ($JO2$) that range from near resting to near maximal. The free energy of ATP hydrolysis can then be determined over this range based on known amounts of creatine (Cr), phosphocreatine (PCr), and ATP. This is done by utilizing excess amounts of creatine kinase (CK) and utilizing the subsequent creatine kinase reaction. Utilizing calculations previously reported, the $\Delta G'_{ATP}$ for each sequential PCr addition was determined [57,58].

Buffer for all assays was Buffer D. All assays were run in a 1mL O2K chamber with 1mL buffer. To this, liver (100μg/mL) mitochondria was added. Once the mitochondria stabilized, energizing substrates were added to the chamber to determine state 4 respiration (non-phosphorylating): Succinate (10mM). Once the mitochondria reached a steady state, clamp substrates were added to the chamber. The substrate conditions were as follows: creatine kinase (50U/mL), phosphocreatine (0.05mM), and ATP (5mM). Following the addition of the clamp substrates, sequential PCr additions were performed to gradually reduce the mitochondria back from a highly energized state

with a high *J*O2, to that of a low energy state with a low *J*O2. When plotting the calculated $\Delta G'_{ATP}$ values against that of the measured *J*O2, a linear force-flow relationship can be determined. This linear relationship corresponds to the conductance of the respirators system under these specific substrate conditions.

By manual manipulation of the ATP/ADP ratio by the addition of PCr, the system better mimics the natural conductance of the mitochondria in vivo. By measuring the conductance, it can be determined if there is an increase (decreased slope) or decrease (increased slope) resistance to the respiratory system. [55,57,59].

Mitochondrial ADP Titration:

An ADP titration was done to assess the mitochondria's ability to respond to a metabolic demand[60]. The ADP titration was carried out under saturating substrate conditions: succinate (10mM). ADP was then titrated in to vary the mitochondrial energetic state from that of State 4 (non-phosphorylating) to that of State 3 (phosphorylating).

Inhibitor Profile Assays:

Similarly to the complex specific assay, an inhibitor profile was carried out. This was done to determine the contribution of each complex to the overall rate of oxygen consumption (JO2) using sequential titration of inhibitors. For this assay, liver (100μg) mitochondria weas used. Once the mitochondria had stabilized in the O2K, substrates were titrated in. Mitochondria were first energized with pyruvate (5mM), glutamate (5mM), malate (2mM), succinate (5mM), and octanoyl-carnitine (0.2mM) to allow for State 4 respiration. To reach State 3, ADP (4mM) was

added. Following State 3 respiration, Rotenone (0.5uM) was added to inhibit Complex I. Malonate (5mM) was added to inhibit Succinate Oxidation. Animycin A (0.5μM) was added to inhibit Complex III respiration. Oligomycin (0.5μM) was added to inhibit any added oxygen consumption from Complex V. Carboxyatractyloside, CAT, was used to inhibit the ANT translocator. Cyanide (10mM) was added to inhibit any residual oxygen consumption from Complex IV.

Dehydrogenase Assay:

Using the autofluorescence of NADH and NADPH (Ex:Em 340:450), the enzymatic activity of glutamate dehydrogenase, malate dehydrogenase, pyruvate dehydrogenase, and Complex V were examined as previously described[57,61]. All activity assays were carried out in a 96-well plate. Fluorescence was measured every 60-seconds over a 60-minute period. Enzymatic activity was determined using a standard curve[61].

Statistical Analysis:

All functional assays were reported as mean $\pm$ SEM. Data was normalized to total protein added per experiment calculated for each sample. The final values were expressed as pmol/s/mg protein. Differences between control and treated groups were assessed by one-way ANOVA followed by a Dunnett's multiple comparisons test when applicable using GraphPad Prism 9 software (9.2.0). Any other statistical tests used are described in figure legends. Unless otherwise stated, all statistical significance denoted is as follows: 0.12 (ns), 0.033 (*), 0.002 (**), <0.001 (***). All figures were generated using GraphPad Prism 9 software (9.2.0).

RESULTS

Time effects of acute glucose and fructose gavage on uric acid production

Within 15 min of fructose gavage, uric acid concentration significantly increased in the liver of 8-week-old mice relative to controls (water gavaged) (Figure 2A). Surprisingly, glucose gavage also significantly increased liver uric acid concentration within 15 min. Uric acid levels remained significantly elevated 60 minutes after either fructose or glucose gavage (Figure 2A). There was

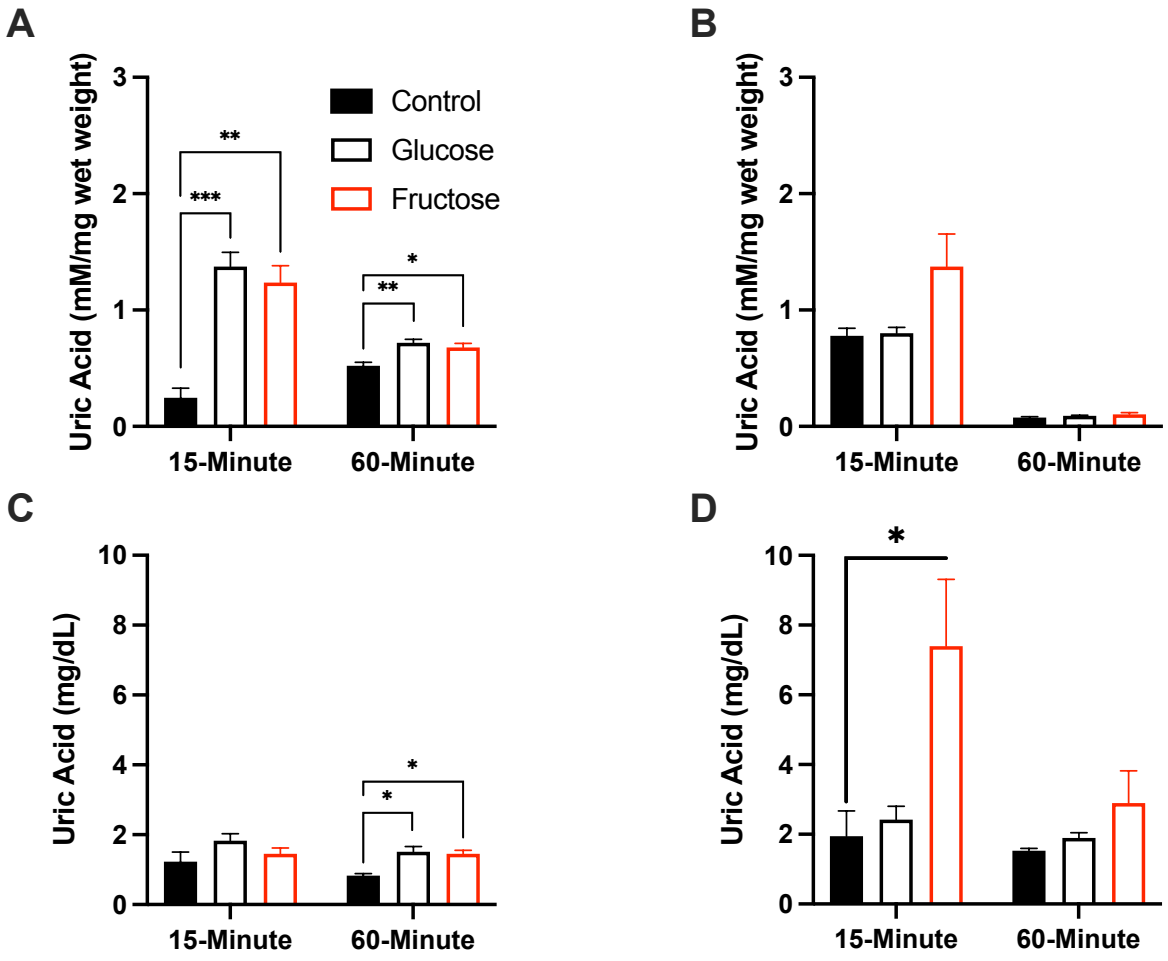

Figure 2: Quantification of uric acid in the liver and blood of acutely gavaged mice. Uric acid concentration in liver tissue (A and B) and blood (C and D) of 8-week-old mice (A and C) and 16-week-old mice (B and D) collected 15-minutes and 60-minutes after gavage. All data is reported as mean ± SEM, N=6**.** All statistical significance denoted is as follows: 0.12 (ns), 0.033 (*), 0.002 (**), <0.001 (***).

no corresponding increase in blood uric acid concentration at 15-min in response to either fructose or glucose gavage (Figure 2C). However, there was a significant increase in uric acid concentration in the blood 60-minutes after either glucose or fructose gavage.

To determine whether the response to acute fructose and glucose gavage is similar in more mature mice, experiments were repeated in 16-week-old mice. Uric acid concentration in response to acute fructose gavage tended to increase ($p=0.069$) in liver and significantly increased in blood within 15 min, but then returned to baseline within 60 min (Figure 2B & 2D). In contrast with 8-week-old mice, glucose gavage in 16-weel-old mice did not affect liver or blood uric acid levels.

Effects of glucose and fructose on mitochondrial respiration

To examine the potential influence of fructose or glucose ingestion on mitochondrial bioenergetics in liver of 8-week-old mice, mitochondria were isolated 15 or 60 min after either fructose of glucose gavage and subjected to force-flow analysis via a creatine kinase clamp[57,61,62]. This assay determines the efficiency of oxidative phosphorylation over a stepwise range of clamped free energies of ATP (i.e., ΔG_{ATP}). At the lowest level of absolute free energy (i.e., -13 ΔG_{ATP}, highest rate of ATP synthesis), the rate of oxygen consumption (JO_2) was significantly greater in mitochondria isolated from liver of mice 15 min after glucose gavage and tended to be higher ($p=0.063$) in fructose gavaged mice relative to controls (Figure 3A). At the next highest level of free energy (-14 ΔG_{ATP}), JO_2 was significantly higher in mitochondria from both fructose and glucose gavaged relative to control mice. Surprisingly after completion of the clamp, addition of FCCP, a mitochondrial uncoupler, failed to restore respiratory capacity, an effect that was more pronounced in controls. This is interesting, as it raises the possibility of an inhibitory effect on flux

through the ETS by adenylate accumulation, which appears more pronounced in control than sugar gavaged mice. Within 60 min after gavage, JO_2 values across the range of ΔG_{ATP} were not different between fructose or glucose gavaged and control animals, although uncoupled respiration was again significantly higher in gavaged mice (Figure 3C).

The response of liver mitochondria to fructose and glucose gavage in 16-week-old mice was quite different. Overall, near maximal clamped ADP-stimulated respiration (i.e., -13 ΔG_{ATP})

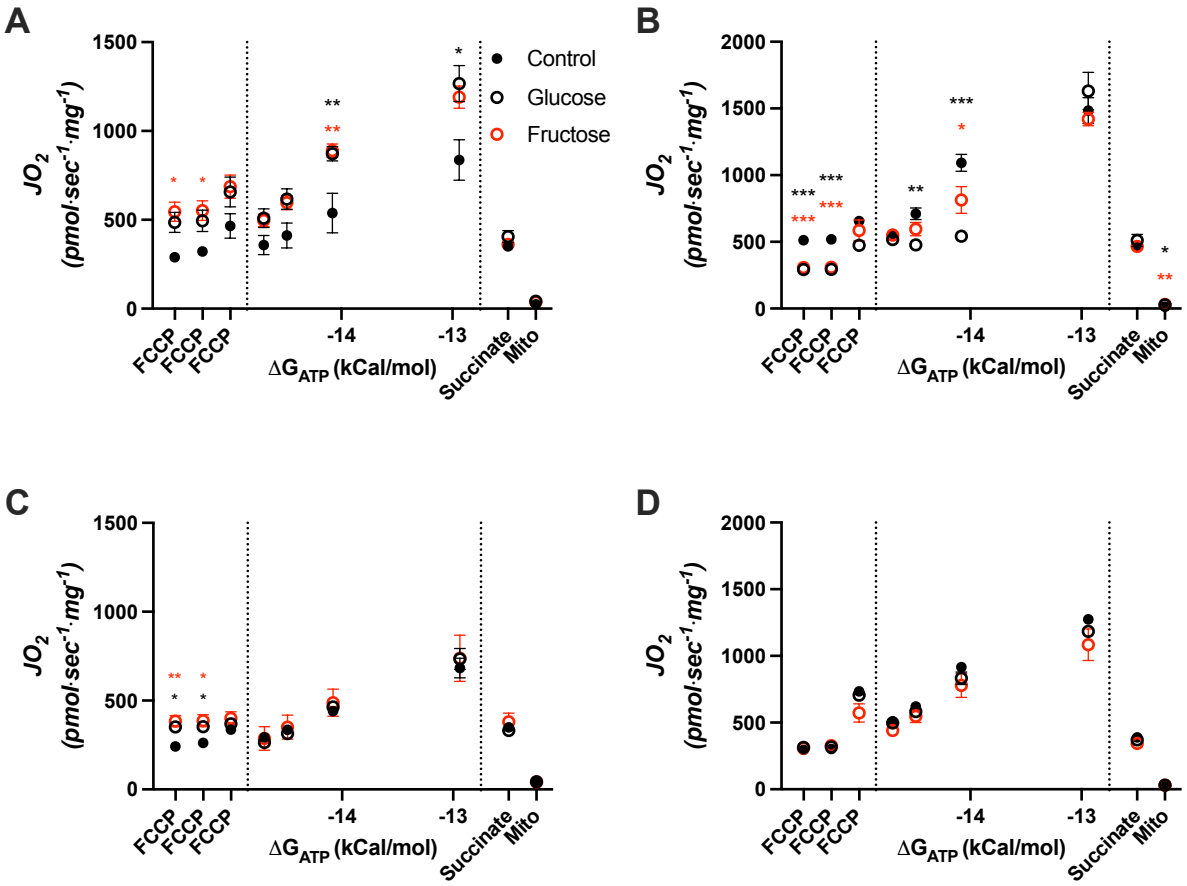

Figure 3: Force-flow analysis of liver mitochondria following an acute gavage. Using the creatine kinase clamp assay, mitochondrial function was determined 15-minutes (A and B) and 60-minutes (C and D) post treatment in 8-week-old mice (A and C) and 16-week-old mice (B and D). All mice were treated with a single gavage and samples were collected 15- and 60-minutes following gavage. All data is reported as mean ± SEM, N=4-6. All statistical significance denoted is as follows: 0.12 (ns), 0.033 (*), 0.002 (**), <0.001 (***). Control vs. glucose comparisons are in black (*) and all control vs. fructose comparisons are in red (*).

was higher in the more mature mice (JO_2 ~1500 vs <1000 pmol•sec^{-1}•mg^{-1} in 16- vs 8-week-old mice). Neither acute fructose nor glucose gavage affected near maximal clamped ADP-stimulated respiration. However, as ΔG_{ATP} increased (≤-14 kCal/mol), JO_2 decreased more rapidly in liver mitochondria from both the fructose- and glucose-gavaged mice (Figure 2B), reflecting a potential allosteric hypersensitivity to the accumulation of adenylate charge. As in 8-week-old mice, addition of FCCP did not elicit a maximal respiratory response in control or fructose/glucose gavaged mice. In fact, JO_2 further decreased in response to FCCP in both the fructose and glucose gavaged mice to rates that were significantly less, not higher, than controls. Again, the impact of fructose or glucose gavage on liver mitochondrial bioenergetics was transient, as no differences were detected 60 min after fructose or glucose gavage relative to controls (Figure 3D).

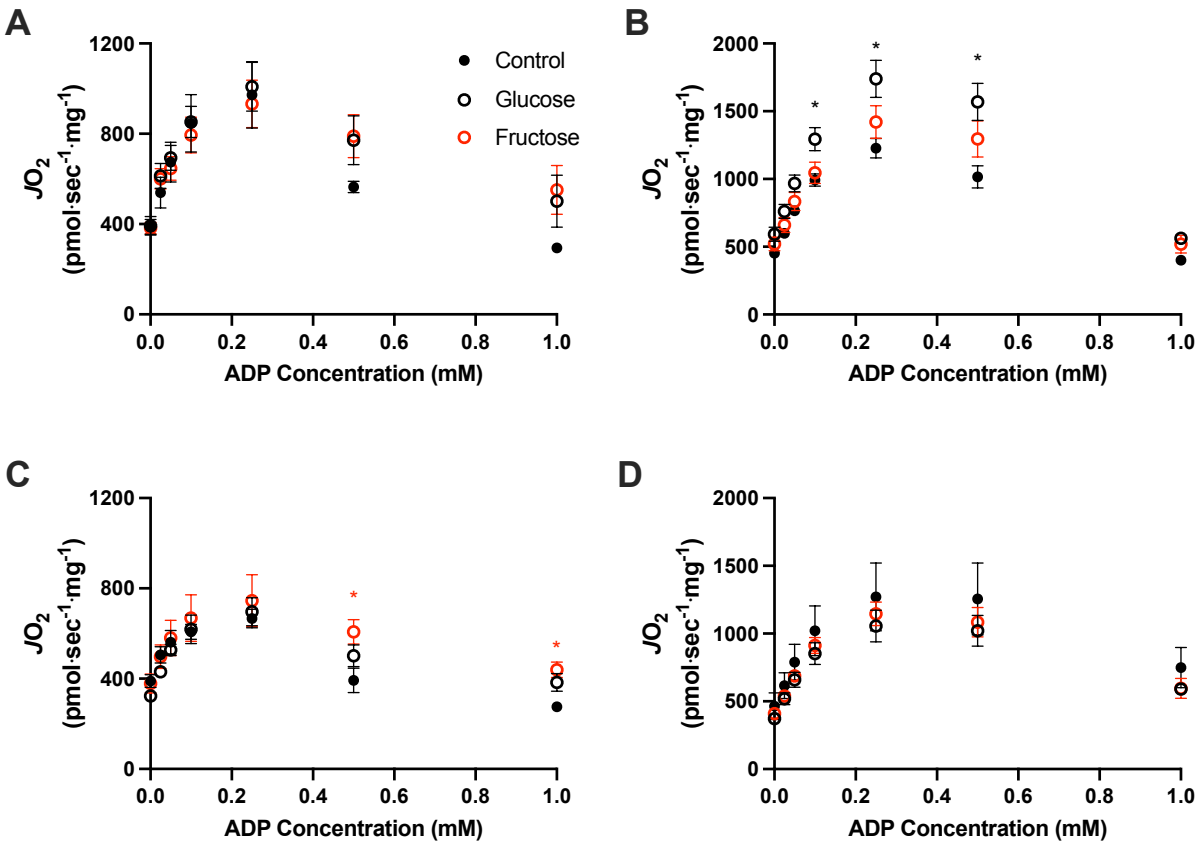

Figure 4: ADP titration of liver mitochondria following an acute gavage. Using an ADP titration, mitochondrial function was determined 15-minutes (A and B) and 60-minutes (C and D) post treatment in 8-week-old mice (A and C) and 16-week-old mice (B and D). All mice were treated with a single gavage and samples were collected 15- and 60-minutes following gavage. All data is reported as mean ± SEM, N=4-6. All statistical significance denoted is as follows: 0.12 (ns), 0.033 (*), 0.002 (**), <0.001 (***). Control vs. glucose comparisons are in black (*) and all control vs. fructose comparisons are in red (*).

In the force-flow assay, both ΔG_{ATP} and the total adenylate pool build stepwise as a consequence of the creatine kinase clamp system. To directly test the influence of the adenylate pool independent of ΔG_{ATP} on bioenergetics, liver mitochondria were subjected to ADP titration in the absence of a free energy clamp system (ATP does not accumulate in buffer to a high enough concentration to generate sufficient ΔG_{ATP}). In 8-week-old mice, ADP titration elicited a progressive increase in JO_2 peaking at 0.25mM. JO_2 then precipitously declined to levels at or

below baseline (Figure 4A). In mitochondria isolated from liver of mice 15 min after either fructose of glucose gavage, JO_2 tended to be higher than controls, consistent with the force-flow data (Figure 3A). At 60-minutes, it is seen that there is a lingering, yet significant, increase in JO_2 at the highest ADP concentrations (Figure 4C). When isolated from 16-week-old mice, the same gradual increases in JO_2 were observed, yet there was a significant increase in the JO_2 of mice gavaged with glucose (Figure 4B). Again, this increase is transient, in which there is no differences detected at 60-minutes post gavage (Figure 4D).

Effects of chronic glucose and fructose treatment on weight and uric acid production

To determine if a chronic gavage with either fructose or glucose was sufficient to elicit changes in mitochondrial bioenergetic function, a 14-day plan was used. Mice were weighed daily to determine if there was a difference in body weights associated with a specific sugar. There was no significant difference in weight between the treatment groups over the 14-day treatment in 8-week-old mice (Figure 5). Surprisingly, after repeated gavage, there was no immediate (15-minute) or delayed (60-minute) increase in uric acid concentration within the liver (Figure 6A) or the blood (Figure 6B). This indicated that there was a protective mechanism at play to alleviate the burden in the liver.

Effects of chronic fructose and glucose treatment on mitochondrial respiration

Using the force-flow assay, it was determined that there was an increase in both the glucose and the fructose groups following the addition of adenylates (-13 ΔG_{ATP}) (Figure 7A). Once again, it

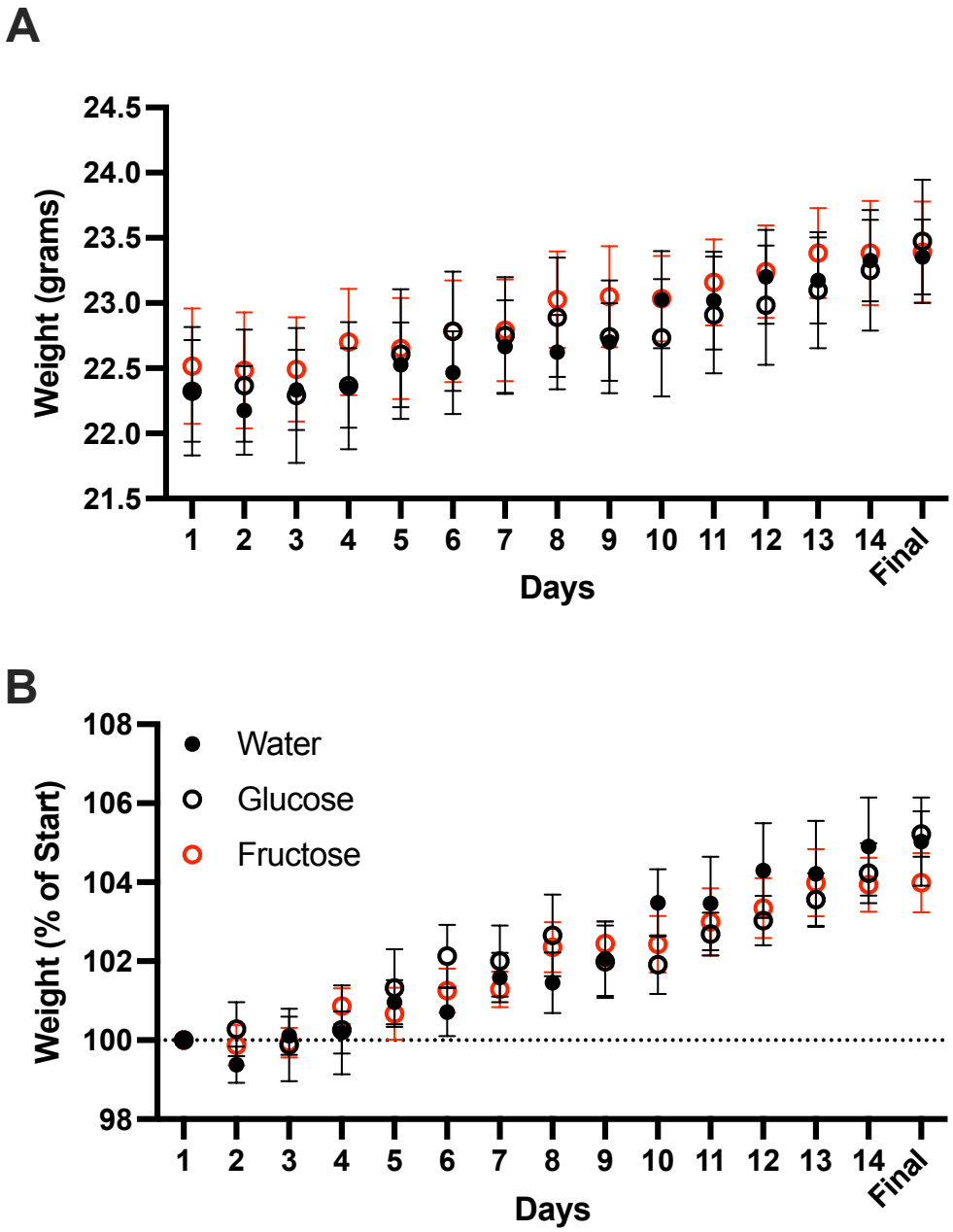

Figure 5: Weight gain curve of all 8-week-old mice over a 14-day treatment period. (A) represents the total weight of the animal in grams where (B) represents the % of weight from the start. All data is reported as mean ± SEM, N=12. All statistical significance denoted is as follows: 0.12 (ns), 0.033 (*), 0.002 (**), <0.001 (***). Control vs. glucose comparisons are in black (*) and all control vs. fructose comparisons are in red (*).

was found that the addition of FCCP to all groups did not elicit a maximal respiratory response to

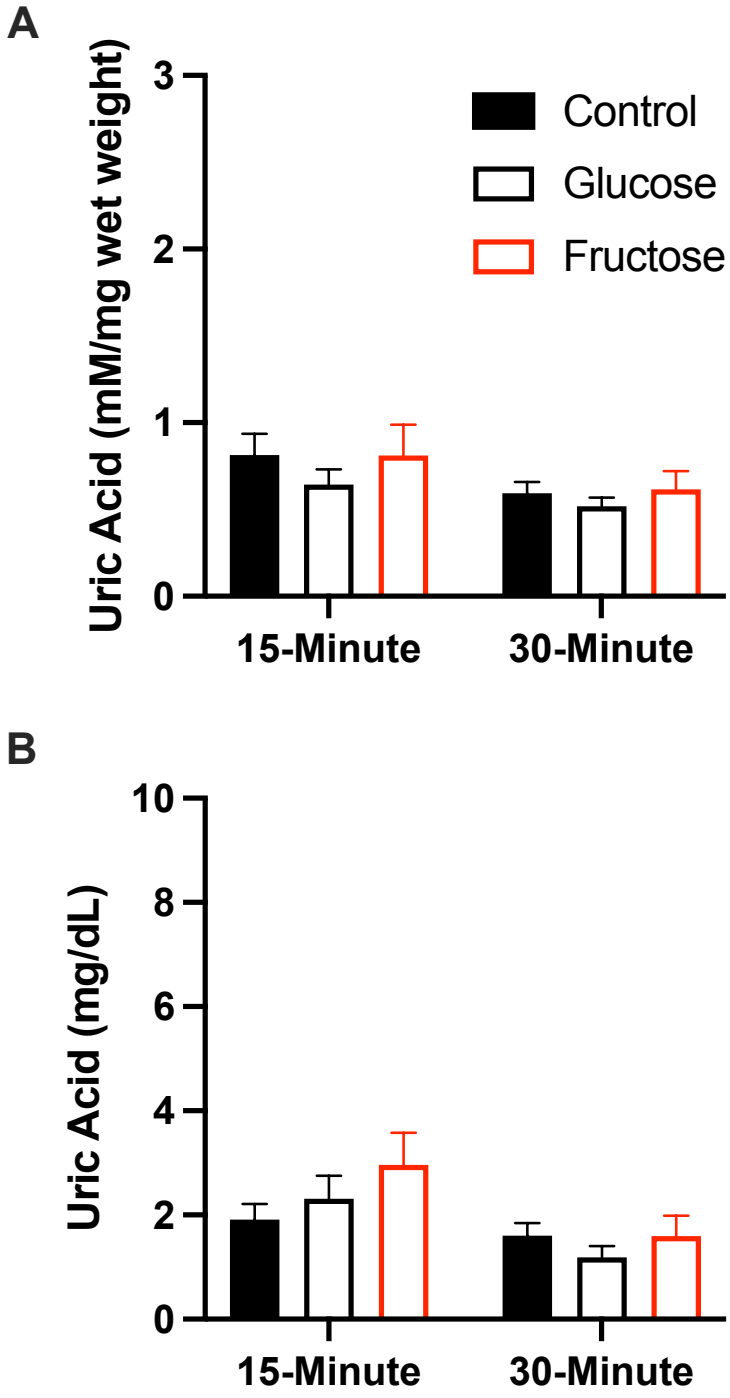

Figure 6: Quantification of uric acid in the liver and blood following a 14-day treatment period. Uric acid concentration in liver tissue (A) and blood (B) of 8-week-old mice treated over a 14-day period collected 15-minutes and 30-minutes after the final gavage. All data is reported as mean ± SEM, N=6. All statistical significance denoted is as follows: 0.12 (ns), 0.033 (*), 0.002 (**), <0.001 (***). Control vs. glucose comparisons are in black (*) and all control vs. fructose comparisons are in red (*).

that of the state 3, ADP stimulated response. Again, this suggests that the presence of adenylates is acting in an inhibitory manner on flux through the ETS system. This finding was transient, in which it was found only within 15-minutes post gavage, and there were no differences detected at 60-minutes post gavage.

It is of note that the ADP titration showed no differences between groups at any time following gavage (Figure 7C and 7D). This, along with the lack of uric acid production, support the notion that a protective mechanism is at work.

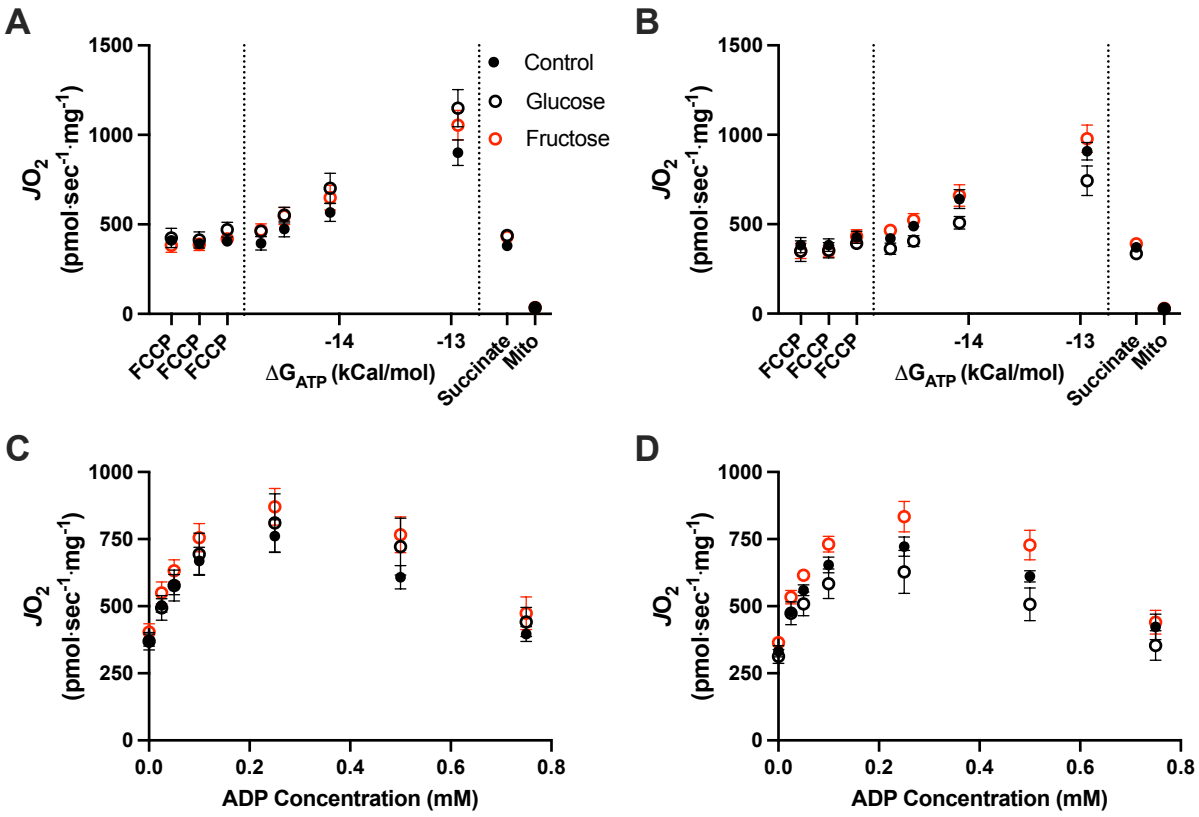

Figure 7: Mitochondrial respiration of liver mitochondria taken from 8-week-old mice following a 14-day treatment period. The creatine kinase clamp assay was utilized in mitochondria 15-minutes (A) and 30-minutes (B) after gavage. An ADP titration was utilized in mitochondria 15-minutes (C) and 30-minutes (D) after gavage. All data is reported as mean ± SEM, N=6. All statistical significance denoted is as follows: 0.12 (ns), 0.033 (*), 0.002 (**), <0.001 (***). Control vs. glucose comparisons are in black (*) and all control vs. fructose comparisons are in red (*).

DISCUSSION

The acute treatment of both fructose and glucose in 8-week-old mice led to a significant increase in uric acid within the liver tissue 15-minutes following the gavage (Figure 2A). The mitochondrial function data, both the clamp (Figure 3A) and the ADP titration (Figure 4A), indicated an increase in JO_2 at the 15-minute time point as well. When taken together, both the concentration data and the mitochondrial data indicated that when acutely treated with either fructose or glucose, there is an immediate shift in liver metabolism, i.e., an increase in flux through the purine degradation pathway, resulting in an increase in uric acid production within the liver.

By the 60-minute time point, there were no differences in the uric acid concentration (Figure 2A) or in the functional outcomes (Figures 3C and 4C) in 8-week-old mice. This supports the idea that uric acid is in fact the driving factor behind the increase in JO_2. Since there is no increase in uric acid production from the liver, there is no increase in rate in the mitochondria.

Unlike the 8-week-old mice, there was no significant increase in uric acid concentration in the liver tissue of 16-week-old mice 15-minutes after a gavage with either fructose or glucose (Figure 2B). This could indicate that the uric acid produced in the liver passes into the blood at a higher rate in 16-week-old mice than in 8-week-old mice. This is evidenced by a significant increase in uric acid concentration in the blood (Figure 2D) but not liver (Figure 2B) 15-minutes after treatment in the 16-week-old mice. Once in the blood, uric acid does not elicit the same bioenergetic effects seen in the 8-week-old mice. This is to say that since the uric acid is no longer present in the liver tissue, there is no subsequent increase in JO_2 in the mitochondria 15-minutes after treatment (Figure 3B and 4B). However, there is a significant drop in JO_2 of the glucose

treated group 15-minutes following treatment (Figure 3B). This drop accompanies the addition of PCr to the system, which in turn leads to an increase in the ATP:ADP ratio. Since additional PCr is not sufficient to change the JO_2 of the glucose treated group even further, it is possible that the presence of ATP in the system is acting in an inhibitory manner. This is to mean that the presence of ATP in a glucose stimulated system acts against the mitochondrial system itself to inhibit OHPHOS[61]. This is further supported by the titration of ADP alone into the system (Figure 4B). A significant increase in JO_2 of the glucose treated group is seen at every ADP addition. This indicates that the mitochondria exposed to a glucose treatment are less efficient, and therefore must work harder, i.e., consume more oxygen, to meet the same ADP demand (Figure 4B). Again, these observed findings are only found within 15-minutes following treatment. By the 60-minute point, there are no longer differences in mitochondrial function between the groups (Figures 3D and 4D).

An interesting finding from all force-flow data was that the addition of FCCP, a mitochondrial uncoupler, does not elicit an increase in JO_2 beyond that of the succinate supported respiration rate (Figure 3). A possible explanation for this is the use of succinate alone as a substrate. With only succinate dehydrogenase driving flux, the addition of FCCP and the subsequent uncoupling of the JO_2 from the OXPHOS system, could potentially crash the membrane potential within the mitochondria, leading to a minimal increase in JO_2 due to substrate limitation[61,63]. All force-flow data supports this due to the lack of increase of JO_2 beyond that of the succinate supported rate. The 16-week-old mice treated with both glucose and fructose exhibit a decrease in JO_2 following FCCP addition (Figure 3B). This can be explained by the combination of ATP inhibition on the respiration rate being further limited by substrate availability.

Interestingly, there was no difference between the weights of the 8-week-old mice subjected to a 14-day treatment with either fructose or glucose (Figure 5). This was accompanied by no change in the production of uric acid in the livers of the treated mice at either 15-minutes or 30-minutes post final gavage (Figure 6). When the mitochondria itself was examined, there were no differences found between the treatment groups following an increase in the JO_2 of the glucose treated group following the addition of nucleotides 15-minutes after the final treatment (Figure 7A). This together suggests that there was an adaptive mechanism involved that protected the overall bioenergetic function of the mice when chronically exposed to both glucose and fructose.

CONCLUSION

All data together conclusively found that only a single gavage was sufficient to elicit a response in the isolated mitochondria. This effect is only seen within 15-minutes following a single gavage. However, the bioenergetic changes seen in this study can be explained by the presence of uric acid. This is evidenced by the increase in JO_2 following the increase in uric acid concentration in the liver. Further studies must be done to determine the amount of added oxygen consumption that can be attributed to urate oxidase. Inhibition of urate oxidase with its known inhibitor, potassium oxonate (KOX) can determine if there is residual impact on mitochondrial function. This study also found that the age of the mice, i.e., 8-week vs 16-week-old, is an important consideration.

CHAPTER 3: Impact of direct uric acid exposure on the bioenergetics of both liver and heart mitochondria

INTRODUCTION

Approximately 66% of Americans are clinically overweight, including about 30% of American children[19]. There is also a correlating rise in obesity related conditions such as metabolic syndrome, type 2 diabetes, nonalcoholic fatty liver disease, and heart disease[19]. While there is no single factor responsible for the increasing prevalence of obesity related disease, fructose has been identified as playing an important role[12,19,33].

Fructose is a monosaccharide sugar used primarily as high-fructose corn syrup or sucrose in processed food sources[12]. Once absorbed into the portal blood, fructose is transported to the liver where it is metabolized[12]. There is a rapid uptake and subsequent phosphorylation of fructose to fructose-1-phosphate (F1P) by ketohexokinase[28]. Unlike glucose metabolism, in which further phosphorylation of glucose is inhibited by the presence of glucose-6-phosphate, F1P does not inhibit the further phosphorylation of fructose. This unregulated phosphorylation and utilization of ATP leads to a rapid decline in the available ATP within the cell. Due to the shift in energy balance, the system then favors the purine degradation pathway, the product of which is uric acid[12,19,20,33,64].

Recently, the presence of uric acid in serum has been used to predict the development of obesity and diabetes[15]. It is known that fructose consumption leads to an increase in uric acid as well as a decrease in ATP levels within the liver[12,19]. Since mitochondria are the main ATP

producers within the cell, mitochondrial function is the focus of this study. Therefore, to fully determine the relationship between the presence of uric acid and the decline of mitochondrial bioenergetic function, resulting in a decline in available ATP, the following experiments were designed: P/O assay, force-flow assay, ADP titration, complex specific assay, and an inhibitor profile. The overall hypothesis is that in the presence of uric acid, there will be a decline in the liver mitochondrial bioenergetic function.

RESEARCH DESIGN AND METHODS

Buffers:

Buffer A: 50mM MOPS buffer supplemented with 100mM KCl, 1mM EGTA, and 5mM $MgSO_4$, pH 7.1, stored at 4°C.

Buffer B: 50mM MOPS buffer supplemented with 100mM KCl, 1mM EGTA, 5mM $MgSO_4$, and 0.2% BSA, pH 7.1, stored at 4°C.

Buffer C: 105mM MES Potassium salt supplemented with 30mM KCl, 1mM EGTA, 10mM Potassium Phosphate (monobasic), 5mM Magnesium Chloride, 0.25% BSA, pH 7.2, stored at 4°C.

Buffer D: 105mM MES Potassium salt supplemented with 30mM KCl, 1mM EGTA, 10mM Potassium Phosphate (monobasic), 5mM Magnesium Chloride, 0.25% BSA, and 5mM Creatine monohydrate, pH 7.2, stored at 4°C.

Buffer E: Buffer C supplemented with 1U/mL of hexokinase, 2U/mL glucose-6-dehydrogenase phosphate, 4mM $NADP^+$, and 5mM glucose.

Animals:

All animal studies were approved by the East Carolina University Institutional Animal Care and Use Committee. C57BL/6NJ male mice were purchased from Jackson Laboratory. All mice were housed in a temperature (22°C) and light controlled (12-hour light/12-hour dark) room and given free access to food and water. Unless otherwise stated, mice were anesthetized with isoflurane before tissue removal.

Chemicals:

Unless otherwise stated, all chemicals were purchased from Sigma-Aldrich.

Mitochondrial Isolation:

Once tissue was removed, it was placed in approximately 15mL ice-cold Buffer B. The tissue was then homogenized for approximately 10 passes using a Teflon pestle and borosilicate glass vessel. The homogenized solution was then transferred to a 50mL Falcon tube, and the volume was brought to approximately 30mL. The homogenate was then spun at 800 x G for 10 minutes at 4°C. The subsequent supernatant was then poured through two layers of gauze into a second 50mL Falcon tube, and the volume was then adjusted to approximately 40mL using Buffer A. The solution was then spun again at 10,000 x G for 10 minutes at 4°C. Following the spin, the supernatant was discarded, and the subsequent pellet was washed with 1.4mL of ice-cold Buffer A. The solution was transferred into a 1.7mL tube before being spun again at 10,000 x G for 10 minutes at 4°C. Following this spin, the supernatant was again discarded, and the final pellet was resuspended in 1mL ice-cold Buffer A. A Pierce BCA assay was then performed on the final solution to determine protein content. Functional assays involving the isolated mitochondria were then carried out in Buffer D [52–54].

Respiration Assays:

Unless otherwise stated, all mitochondrial respiration assays were carried out in Buffer D.

Mitochondrial Uric Acid Titration:

A uric acid titration was used to determine the experimental uric acid dose to be used in subsequent experiments. Heart (50μg) and liver (100μg) mitochondria were energized with pyruvate (5mM), glutamate (5mM), malate (2mM), succinate (5mM), octanoyl-carnitine (0.2mM). Both state 3 and state 4 conditions were tested in parallel. State 3 respiration was reached with the addition of 4mM ADP. Sequential uric acid additions were made to determine the resulting increase in oxygen consumption rate (JO_2). To determine if there was a time-dependent factor involved, control mitochondria were run in parallel to the treated.

Mitochondrial P/O:

To determine the efficiency of mitochondria exposed to uric acid, a P/O ratio was determined. This was done with heart (20μg/mL) and liver (75μg/mL) mitochondria. All mitochondria were energized with pyruvate (5mM), glutamate (5mM), malate (2mM), succinate (5mM), octanoyl-carnitine (0.2mM). Additional P1,P5-di(adenosine-5′) pentaphosphate (AP5A) (0.1mM) was used to inhibit any adenylate kinase present. All assays were run using Buffer E as previously described. *J*O2 and *J*ATP were measured in parallel using an O2K (*J*O2) and a fluorometer (*J*ATP)[61].

Mitochondrial Substrate Oxidation:

To determine mitochondrial substrate preference, multi-substrate and fatty acid substrate conditions were performed. Both assays utilized liver (75μg) and heart (50μg) mitochondria. The

multi-substrate condition was then energized with pyruvate (5mM), glutamate (5mM), malate (2mM), succinate (5mM), and octanoyl-carnitine (0.2mM). The lipid condition utilized palmitoyl-CoA (PCoA) (0.02mM), malate (0.5mM), palmitoyl-carnitine (PC) (0.018mM), and carnitine (5mM). Following the substrate addition, ADP (4mM) was added to both conditions. The lipid condition then received additional electron transport substrates, pyruvate (5mM), glutamate (5mM), and succinate (10mM). FCCP was added to determine maximal uncoupled respiration.

Mitochondrial Respiratory Control:

All mitochondrial respiration measurements were made using a high resolution Oxygraph-2K (Oroboros Instruments) at 37°C. To measure the respiratory control of the mitochondria, a modified version of the creatine kinase clamp assay was utilized [55,56]. This assay utilizes steady-state oxygen consumption rates (*J*O2) that range from near resting to near maximal. The free energy of ATP hydrolysis can then be determined over this range based on known amounts of creatine (Cr), phosphocreatine (PCr), and ATP. This is done by utilizing excess amounts of creatine kinase (CK) and utilizing the subsequent creatine kinase reaction. Utilizing calculations previously reported, the $\Delta G'_{ATP}$ for each sequential PCr addition was determined [57,58].

Buffer for all assays was Buffer D. All assays were run in a 1mL O2K chamber with 1mL buffer. To this, liver (75μg/mL) and heart (50μg/mL) mitochondria were added. Once the mitochondria stabilized, energizing substrates were added to the chamber to determine state 4 respiration (non-phosphorylating): pyruvate (5mM), glutamate (5mM), malate (2mM), succinate (5mM), and octanoyl-carnitine (0.2mM). Once the mitochondria reached a steady state, clamp substrates were added to the chamber. The substrate conditions were as follows: creatine kinase (50U/mL for liver

and 20U/mL for heart), phosphocreatine (0.05mM), and ATP (5mM). Following the addition of the clamp substrates, sequential PCr additions were performed to gradually reduce the mitochondria back from a highly energized state with a high *J*O2, to that of a low energy state with a low *J*O2. When plotting the calculated $\Delta G'_{ATP}$ values against that of the measured *J*O2, a linear force-flow relationship can be determined. This linear relationship corresponds to the conductance of the respiratory system under these specific substrate conditions.

By manual manipulation of the ATP/ADP ratio by the addition of PCr, the system better mimics the natural conductance of the mitochondria in vivo. By measuring the conductance, it can be determined if there is an increase (decreased slope) or decrease (increased slope) resistance to the respiratory system. [55,57,59].

Mitochondrial ADP Titration:

An ADP titration was done to assess the ability of mitochondria to respond to a metabolic demand[60]. The ADP titration was carried out under saturating substrate conditions, pyruvate (5mM), glutamate (5mM), malate (2mM), succinate (5mM), and octanoyl-carnitine (0.2mM). ADP was then titrated in to vary the mitochondrial energetic state from that of State 4 (non-phosphorylating) to that of State 3 (phosphorylating).

Mitochondrial Complex Specific Assays:

All complex specific measurements were made using an O2K using isolated mitochondria in buffer D at 37°C to determine the contribution of each aspect of the electron transport system. Both liver (75μg) and heart (50μg) mitochondria were used. To measure the respiration in complex 1, 2 and

4, the following workflow was utilized. Once the mitochondria had reached a steady state in the O2K, glutamate (5mM) and octanoyl-carnitine (0.2mM) were added, followed by ADP (4mM), then pyruvate (5mM) and malate (5mM) to initiate State 3 respiration through Complex I. To allow for flux through Complex II and the subsequent remainder of the full system, succinate was then added (5mM). To determine the oxygen consumption rate attributed to Complex II, rotenone (0.005mM) was added to inhibit Complex I. Complex IV respiration was determined by adding malonate (5mM) to inhibit succinate oxidation and Antimycin A (0.5uM) to inhibit Complex III, then adding N, N, N′, N′-tetramethyl- p -phenylenediamine (TMPD) (0.5mM) along with Ascorbate (2mM). Complex III determination was done with isolated liver (75μg) and isolated heart (50μg) mitochondria and with the addition of ADP (4mM) along with Duroquinol (0.5mM). Following the reaction, Antimycin A (0.25uM) was added to determine the rate of oxygen consumption that was non-specific to Complex III [65,66].

Inhibitor Profile Assays:

Similarly to the complex specific assay, an inhibitor profile was carried out. This was done to determine the contribution of each complex to the overall rate of oxygen consumption using sequential titration of inhibitors. For this assay, both liver (75μg) and heart (50μg) mitochondria were used. Once the mitochondria had stabilized in the O2K, substrates were titrated in. Mitochondria were first energized with pyruvate (5mM), glutamate (5mM), malate (2mM), succinate (5mM), and octanoyl-carnitine (0.2mM) to allow for State 4 respiration. To reach State 3, ADP (4mM) was added. Following State 3 respiration, Rotenone (0.5uM) was added to inhibit Complex I. Malonate (5mM) was added to inhibit Succinate Oxidation. Antimycin A (0.5uM) was added to inhibit Complex III respiration. Oligomycin (0.5uM) was added to inhibit any added

oxygen consumption from Complex V. Cyanide (10mM) was added to inhibit any residual oxygen consumption from Complex IV.

Mitochondrial Uncoupling vs. Urate Oxidase:

Heart (50μg) and liver (100μg) mitochondria were energized with pyruvate (5mM), glutamate (5mM), malate (2mM), succinate (5mM), octanoyl-carnitine (0.2mM). Once again, both state 3 and state 4 conditions were tested in parallel. State 3 respiration was reached with the addition of 4mM ADP. Uric acid (0.2mM) was then added. To determine if the source was due to proton conductance through uncoupling, Antimycin a was used to inhibit oxidative phosphorylation. To determine if the increase was due to a non-mitochondrial source, specifically urate oxidase, the inhibitor potassium oxonate (KOX) was used at a concentration of 9μg/mL.

Statistical Analysis:

All functional assays were reported as mean $\pm$ SEM. Data was normalized to total protein added per experiment calculated for each sample. The final values were expressed as pmol/s/mg protein. Unless otherwise stated, differences between control and treated groups were assessed by one-way ANOVA followed by a Šídák's multiple comparisons test when applicable using GraphPad Prism 9 software (9.2.0). Any other statistical tests used are described in figure legends. Unless otherwise stated, all statistical significance denoted is as follows: 0.12 (ns), 0.033 (*), 0.002 (**), <0.001 (***). All figures were generated using GraphPad Prism 9 software (9.2.0).

RESULTS

Uric acid effect is specific to liver mitochondria.

To determine if uric acid directly impacts mitochondrial function, increasing amounts of uric acid leads to increasing rates of oxygen consumption (Figure 8). This figure (Figure 8) indicates the rate of oxygen consumption following each addition of uric acid. There is an increase in oxygen consumption rate in the liver mitochondria both in the presence (Figure 8A and 8E) and the absence (Figure 8C and 8G) of adenylates. In the heart mitochondria, there was no increase in JO_2 following the addition of uric acid both in the presence (Figure 8B and 8F) and absence (Figure 8D and 8H) of adenylates. An increase in JO_2 in this situation can be explained by one of two mechanisms. The first is that there is increased proton conductance throughout the electron

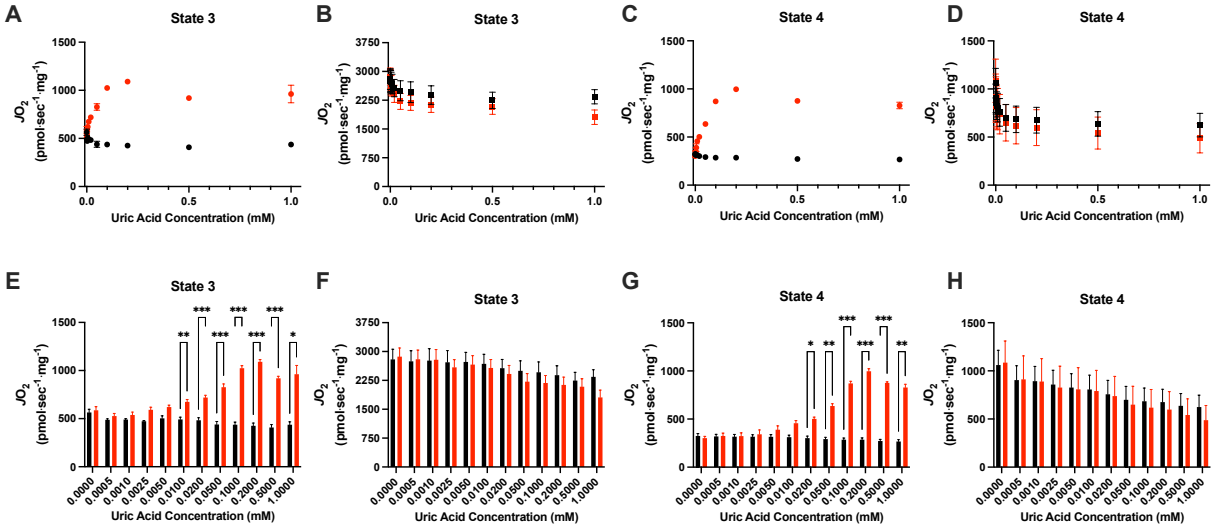

Figure 8: Uric acid dose dependent response curve. Note: This figure represents one data set in two different forms. (A, E) Uric acid titrated into isolated liver (100μg) mitochondria under state 3 conditions. Control conditions utilized mitochondria alone to determine a time dependent change in JO_2. Uric acid treated conditions utilized sequential additions of uric acid as denoted. (B, F) Uric acid titrated into isolated heart (50μg) mitochondria under state 3 conditions. (C, G) Uric acid titrated into isolated liver (100μg) mitochondria under state 4 conditions. (D, H) Uric acid titrated into isolated heart (50μg) mitochondria under state 4 conditions. All mitochondria were energized with pyruvate (5mM), glutamate (5mM), malate (2mM), succinate (5mM), and octanoyl-carnitine (0.2mM). State 3 respiration was reached with the addition of ADP (4mM). Data is represented as mean $\pm$ SEM, N= 3. All statistical significance denoted is as follows: 0.12 (ns), 0.033 (*), 0.002 (**), <0.001 (***).

transport system within the mitochondria itself. The second is that there is a non-mitochondrial factor contributing to the increase in oxygen consumption. With no changes in the JO_2 of heart mitochondria, the effect is liver mitochondria specific. Figure 8 also indicates 0.2mM uric acid elicits the maximum increase in JO_2. Based on this finding, all subsequent experiments used 0.2mM uric acid.

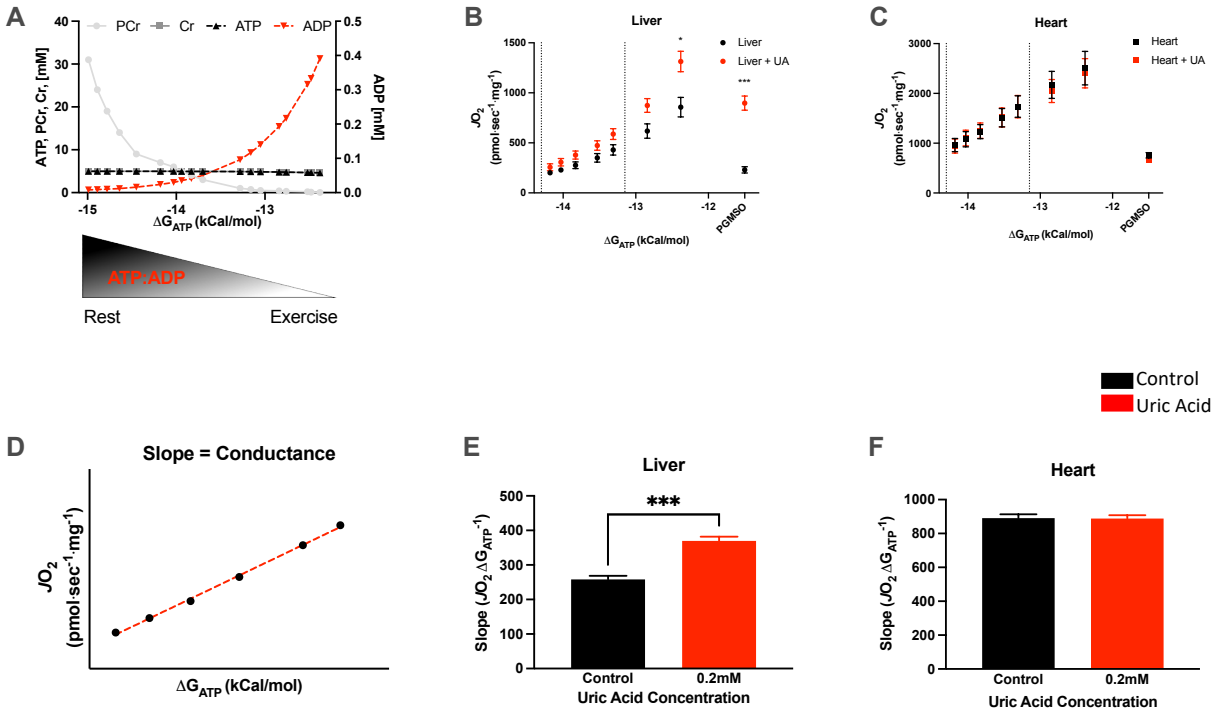

Figure 9: Uric acid addition leads to an increased oxygen consumption rate. (A) Graphical representation of the creatine kinase clamp assay conditions. The assay moves from right to left with sequential PCr additions, which varies the ATP:ADP ratio by decreasing the ADP concentration within the system[57]. (B) The response of isolated liver mitochondria (100μg) across the range of ADP-stimulated steady states. (C) The response of isolated heart mitochondria (50μg) across the range of ADP-stimulated steady states. (D) Graphical representation of the general meaning of the slope of the linear region of the creatine kinase clamp region[57]. (E) Calculated slope of the linear region of the liver mitochondria. (F) Calculated slope of the linear region of the heart mitochondria. All mitochondria were energized with pyruvate (5mM), glutamate (5mM), malate (2mM), succinate (5mM), and octanoyl-carnitine (0.2mM). Uric acid was given at a final concentration of 0.2mM. Data is represented as mean $\pm$ SEM, N= 8-9. All statistical significance denoted is as follows: 0.12 (ns), 0.033 (*), 0.002 (**), <0.001 (***).

Uric acid exposure induces increased oxygen consumption in liver mitochondria regardless of energetic demand.

The uric acid titration was done at a single ADP concentration, so to determine if there was an increase in JO_2 across a range of steady-state ADP-stimulated rates, the creatine kinase system was used (Figure 9A). In this system, known concentrations of creatine kinase (CK), creatine (Cr), phosphocreatine (PCr), and ATP are added to the system (Figure 9A). This system utilizes the creatine kinase reaction in which ADP levels are varied from high (similar to that during exercise) to low (similar to that during rest) by titrating in PCr. With the ATP concentration held constant, the change in ADP concentration led to a shift in the overall ATP:ADP ratio (Figure 9A). This assay uncovered a nearly 5-fold increase in oxygen consumption rate of liver mitochondria exposed to uric acid in the absence of nucleotides (Figure 9B). After the addition of nucleotides, there was an increase in JO_2 from 230 pmol/sec/mg with PGMSO to 857 pmol/sec/mg in control mitochondria, as opposed to an increase in JO_2 from 897 pmol/sec/mg with PGMSO to 1312 pmol/sec/mg in the uric acid exposed mitochondria (Figure 9B). Over the course of the PCr titration, as respiratory demand decreased, the difference in rates between the control and uric acid treated decreased, leading to an overall increase in slope in the treated mitochondria (Figure 9D). The overall increase in JO_2 suggests an increase in conductance throughout the electron transport system (Figure 9E). This same pattern was limited to the liver mitochondria and not carried to the heart (Figure 9C and 9F).

To determine if the increase in JO_2 previously seen was dependent upon the energetic demand in the system, an ADP titration was carried out (Figure 10). This was done to determine the impact of uric acid on respiration as the ADP demand was increased. While there was an overall

increase at every ADP addition in the uric acid treated liver mitochondria, the increase in JO_2 was only increased from 1046 pmol/sec/mg with PGMSO to 1135 pmol/sec/mg at the max respiration point, whereas the control mitochondria increased from 340 pmol/sec/mg with PGMSO to 658 pmol/sec/mg at their max JO_2 (Figure 10A). This could suggest that uric acid interferes with liver

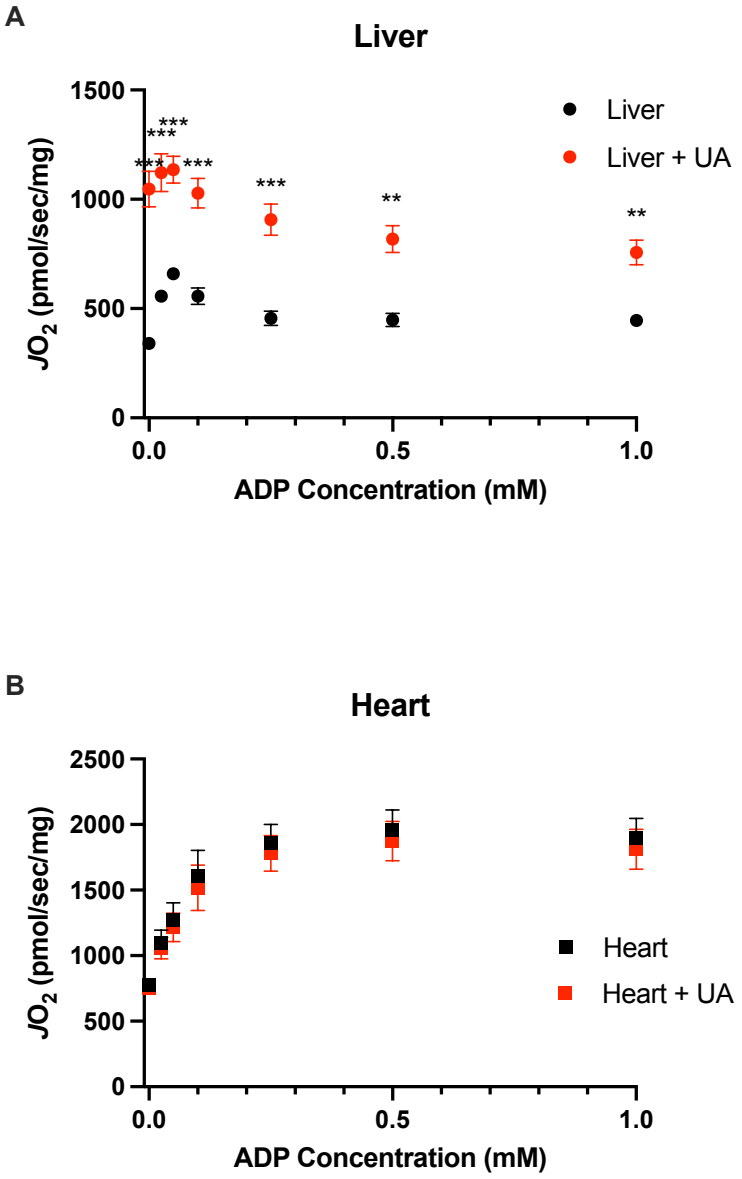

Figure 10: ADP titration of liver and heart mitochondria following uric acid exposure. ADP titration of (A) isolated liver (100μg) and (B) isolated heart (50μg) mitochondria. All mitochondria were energized with pyruvate (5mM), glutamate (5mM), malate (2mM), succinate (5mM), and octanoyl-carnitine (0.2mM). Uric acid was given at a final concentration of 0.2mM. Data is represented as mean ± SEM, N= 10. All statistical significance denoted is as follows: 0.12 (ns), 0.033 (*), 0.002 (**), <0.001 (***).

mitochondria's ability to respond to an ADP demand. It is of note that there is once again no effect in the heart mitochondria (Figure 10B).

Uric acid does not inhibit OXPHOS in liver mitochondria.

To determine if there was an inhibition to oxidative phosphorylation, a P/O ratio was determined (Figure 11). This assay revealed that there was no significant change in the rate of ATP production in the liver mitochondria exposed to uric acid as compared to that of the control. With this, it can be said that uric acid exposure is not directly linked to an inhibition of ATP production in the liver (Figure 11A). There was a significant increase in the oxygen consumption rate of the liver mitochondria exposed to uric acid (Figure 11C). When analyzed as a ratio between rate of ATP production and rate of oxygen consumption, there is a significant decrease in the P/O ratio of liver mitochondria exposed to uric acid (Figure 11E). This supports the previous finding of either increased conductance throughout the OXPHOS system, or increased oxygen consumption through a non-mitochondrial source. The same pattern is not seen in the heart mitochondria (Figure 11B, 11D, and 11F), where there is no difference between the rates of the control sample and the sample exposed to 0.2mM uric acid. In mitochondria isolated from the heart, there was no significant difference found in the JO_2, the JATP, or the P/O ratio between the control and the uric acid treated mitochondria (Figure 12B, 12D, and 12F).

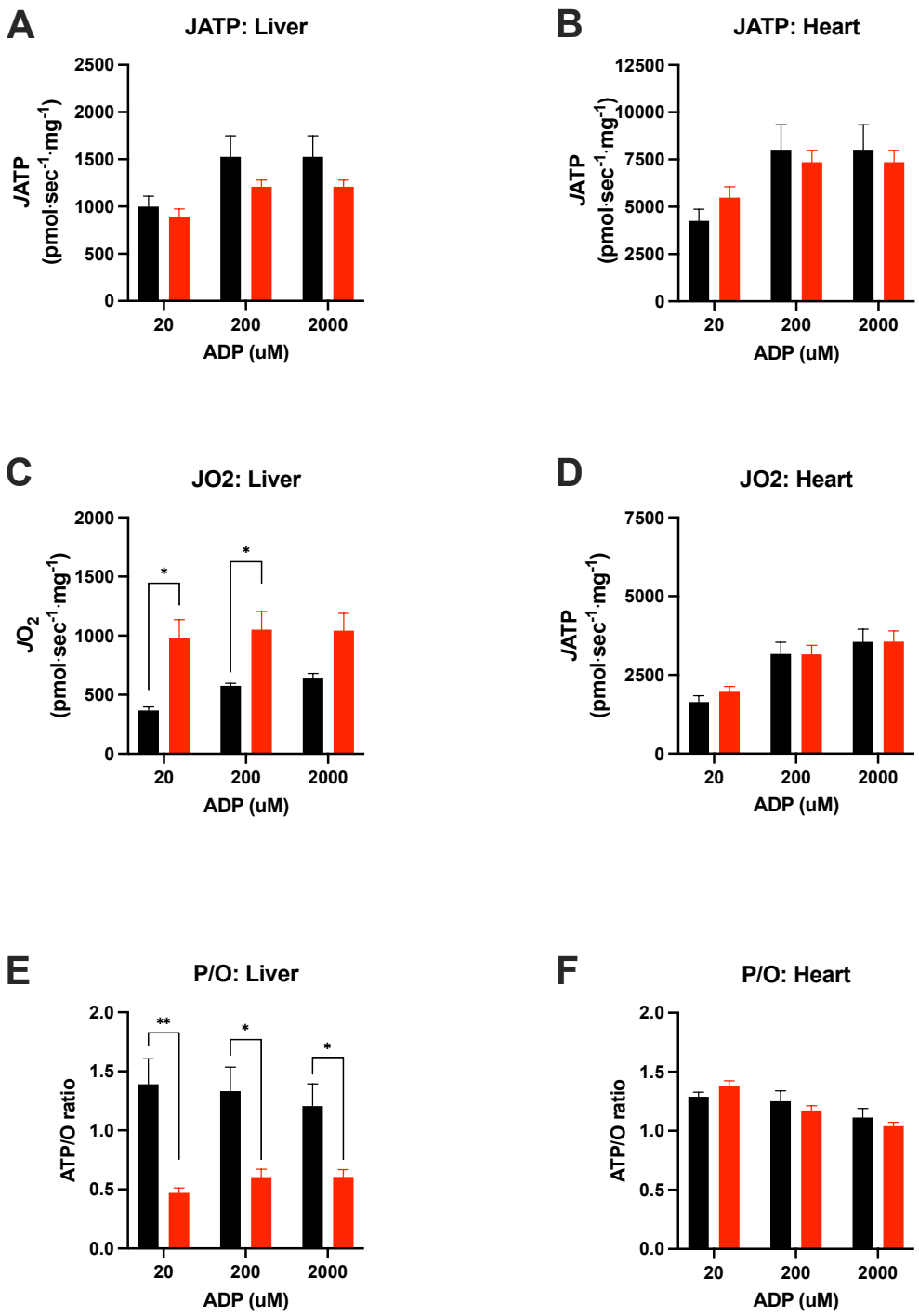

Figure 11: A measure of mitochondrial efficiency as determined by the P/O ratio. All measurements were made in parallel. (A, C, E) Isolated liver mitochondria (75μg/mL) was used to determine the rate of ATP production (JATP), the rate of oxygen consumption (JO_2), and the subsequent ratio of the two. (B, D, F) Isolated heart mitochondria (50μg/mL) was used to determine the rate of ATP production (JATP), the rate of oxygen consumption (JO_2), and the subsequent ratio of the two. All mitochondria were energized with pyruvate (5mM), glutamate (5mM), malate (2mM), succinate (5mM), and octanoyl-carnitine (0.2mM). Uric acid was given at a final concentration of 0.2mM. Data is represented as mean $\pm$ SEM, N= 3. All statistical significance denoted is as follows: 0.12 (ns), 0.033 (*), 0.002 (**), <0.001 (***).

Increased oxygen consumption rate in the presence of uric acid is not linked to increased flux

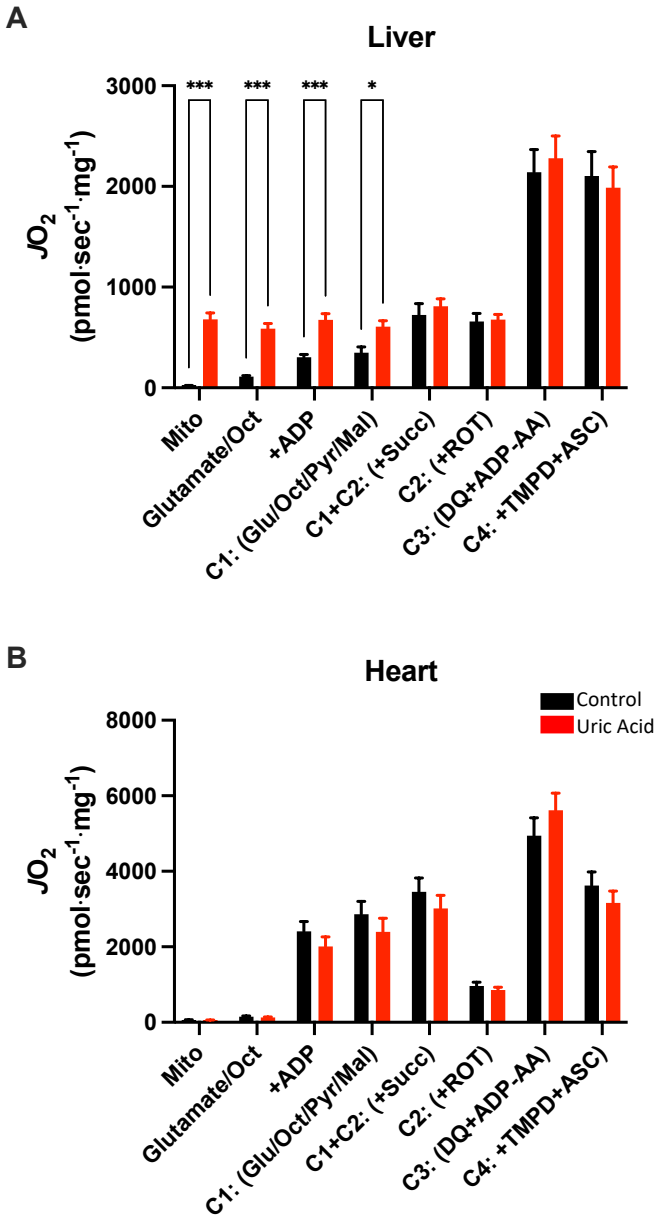

Figure 12: Complex specific breakdown of mitochondrial respiration. (A) Isolated liver (100μg) mitochondria and (B) isolated heart (50μg) mitochondria were used to determine the contribution of each complex to the overall respiration rate (JO_2). The additions were as follows: glutamate (5mM) and octanoyl-carnitine (0.2mM), followed by ADP (4mM) to begin OXPHOS. Then pyruvate (5mM) and malate (5mM) were added to fully initiate State 3 respiration using complex I. Succinate (10mM) was added last followed by rotenone. Respiration was inhibited by antimycin A and oligomycin before the addition of TMPD and Ascorbate. Complex 3 was measured in a separate assay. Uric acid was given at a final concentration of 0.2mM. Data is represented as mean $\pm$ SEM, N= 9. All statistical significance denoted is as follows: 0.12 (ns), 0.033 (*), 0.002 (**), <0.001 (***).

through specific complexes.

A complex specific assay was used to determine if the source of the excess oxygen consumption rate could be identified and linked to a specific complex within the mitochondrial system (Figure 12). It was determined that uric acid exposure increased JO_2 in liver mitochondria in the absence of any substrates (Figure 12A). This increase remained constant throughout the addition of glutamate and ocanoyl-carnitine, with no subsequent increase following an ADP addition. The addition of succinate equalized the oxygen consumption rates of both groups (Figure 12A). This provides further evidence that the added oxygen consumption rates in the liver mitochondria are due to a non-mitochondrial source. The heart mitochondria showed no change in oxygen consumption rate (Figure 12B).

Increased oxygen consumption rates in liver mitochondria in the presence of uric acid suggest an uncoupling effect.

While it was found that there was no inhibition of uric acid on OXPHOS, there was still a large amount of JO_2 unaccounted for. To determine where in the system it was coming from, an inhibitor profile was used (Figure 13). In this assay, it was determined that the addition of uric acid alone to liver mitochondria was sufficient to elicit a maximal increase in JO_2 (Figure 13A). This increase was maintained through the addition of substrates and subsequent ADP to reach state 3 respiration. The addition of Complex I inhibitor rotenone led to no change in respiration for either group. However, the addition of malonate, an inhibitor of succinate oxidation, decreased respiration in both the control and the uric acid group. The drop in JO_2 was seen in both the control and the uric acid group, which indicated that succinate oxidation is required to support the uric acid mediated JO_2. The further addition of Antimycin A (OXPHOS) and Oligomycin (Complex V) show no

further decrease in the control group. Yet there are slight decreases with each in the uric acid group (Figure 13A). This indicated that there was an additional source of oxygen consumption at work within the system. If the increase in JO_2 was due to a single source, there would be no change in rates with each addition past malonate. It is of note that there was no increase in JO_2 in heart mitochondria following the addition of uric acid (Figure 13B).

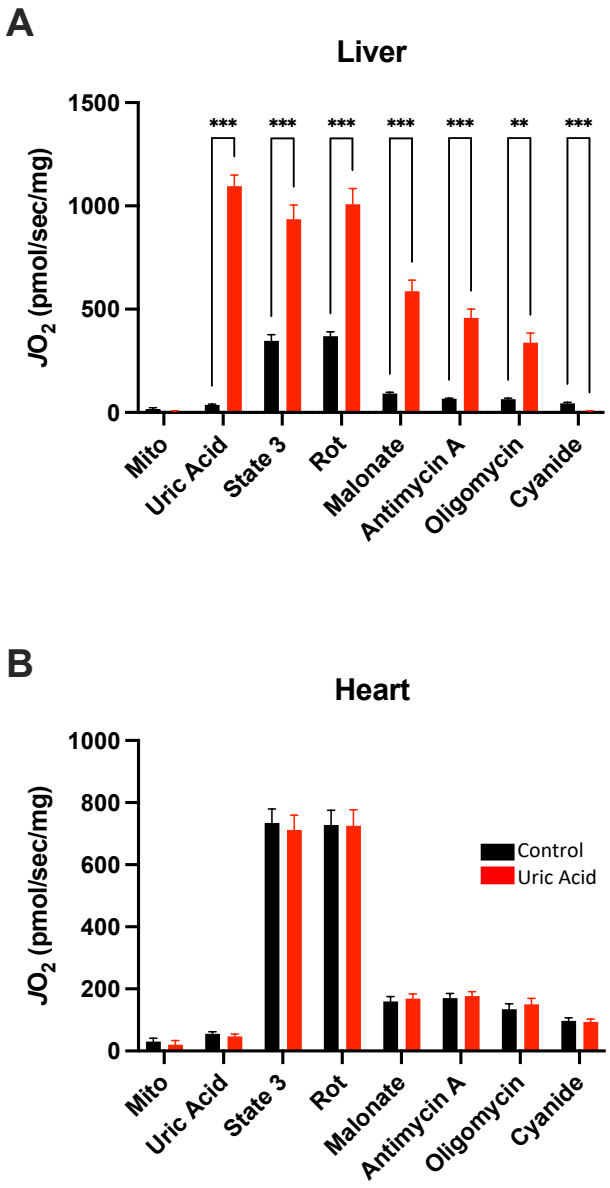

Figure 13: Inhibitor profile to identify source of oxygen consumption. (A) Isolated liver (100μg) mitochondria and (B) isolated heart mitochondria (50μg) were used to determine the potential source of excess oxygen consumption with the mitochondria. State 3 respiration was determined with the addition of pyruvate (5mM), glutamate (5mM), malate (2mM), succinate (5mM), octanoyl-carnitine (0.2mM), and ADP (4mM). The following inhibitors were then added sequentially: Rotenone (0.5μM, Complex I), Malonate (5mM Succinate Oxidation), Antimycin A (0.5μgM, Complex III), Oligomycin (0.5μgM, Complex V), Cyanide (10mM, residual oxygen consumption from Complex IV). Uric acid was given at a final concentration of 0.2mM. Data is represented as mean $\pm$ SEM, N= 9. All statistical significance denoted is as follows: 0.12 (ns), 0.033 (*), 0.002 (**), <0.001 (***).

Increased oxygen consumption: uncoupler vs. oxidase.

With an increase in oxygen consumption rate in a uric acid dose-dependent manner with no subsequent change in rate of ATP production, the question of uncoupler vs oxidase surfaced. To determine the mechanism by which uric acid induced an increase in JO_2, Antimycin A, a known

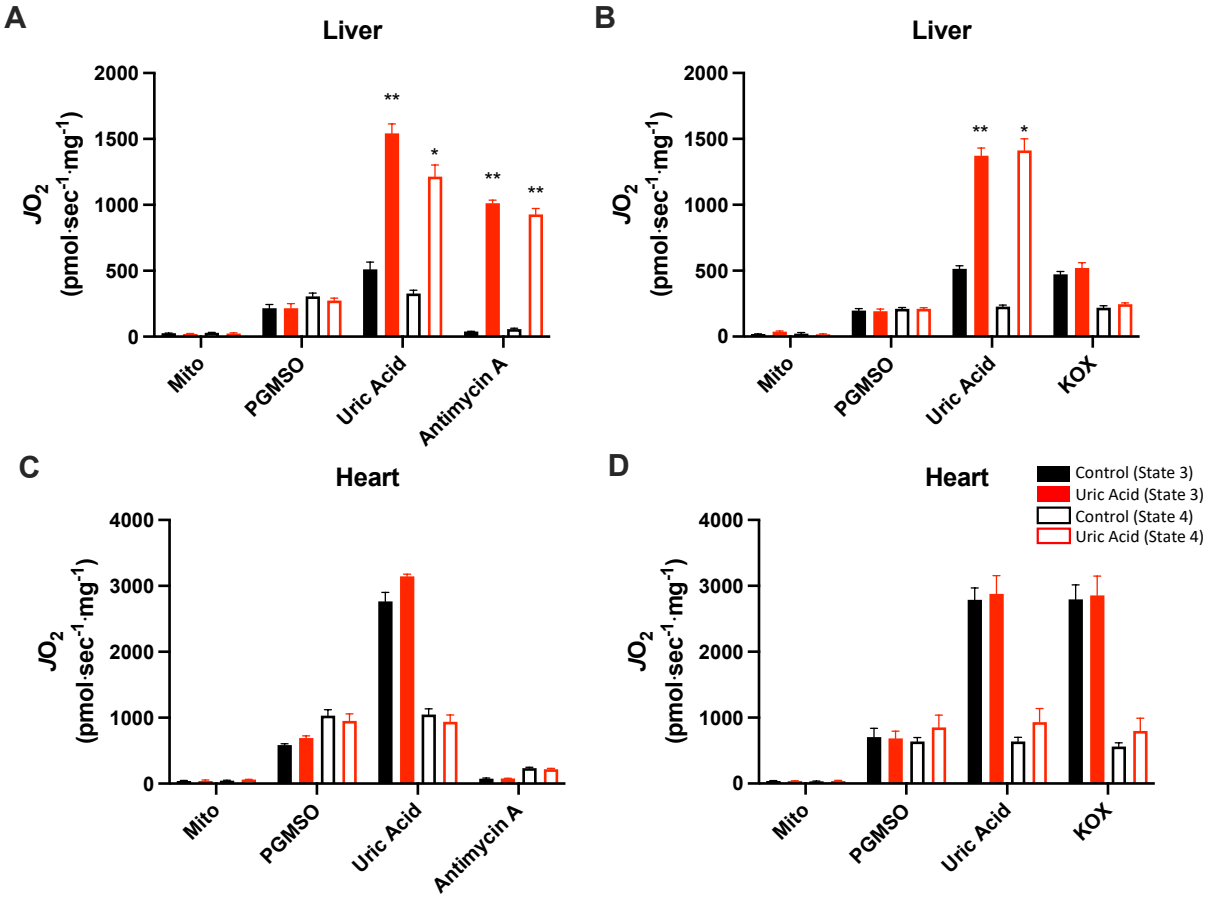

Figure 14: Uncoupling vs Uricase determination. (A,B) Isolated liver (100μg) mitochondria were used to determine if the residual oxygen consumption rate (JO_2) was due to an uncoupling effect or a non-mitochondrial source. (C,D) Isolated heart (50μg) mitochondria were used to determine if the residual oxygen consumption rate (JO_2) was due to an uncoupling effect or a non-mitochondrial source. All mitochondria were energized with pyruvate (5mM), glutamate (5mM), malate (2mM), succinate (5mM), and octanoyl-carnitine (0.2mM). Sate 3 respiration was then determined following an ADP (4mM) addition. Antimycin A was added to inhibit OXPHOS. Potassium oxonate (KOX, 9μg/mL) was used to inhibit urate oxidase. All uric acid was given at a final concentration of 0.2mM. Data is represented as mean $\pm$ SEM, N= 3. All statistical significance denoted is as follows: 0.12 (ns), 0.033 (*), 0.002 (**), <0.001 (***).

OXPHOS inhibitor, was used (Figure 14). Under both state 4 and state 3 respiratory conditions,

an increase in JO_2 was still present in liver mitochondria exposed to 0.2mM uric acid (Figure 14A). It is known that rodents maintain uric acid oxidase within the liver. This reaction further metabolizes uric acid in rodents to a final product of allantoin and requires an additional input of oxygen (Figure 15). To account for this, a second assay was run in which potassium oxonate (KOX), a known urate oxidase inhibitor was used instead (Figure 15). This inhibitor addition was sufficient to reduce the JO_2 in the uric acid treated group back to that of the control group (Figure 7B). This confirmed that the increased rate of oxygen consumption seen in liver mitochondria treated with uric acid is due to oxygen consumption by urate oxidase. The addition of uric acid to heart mitochondria did not change the rate of oxygen consumption. The addition of Antimycin A fully inhibited all oxygen consumption (Figure 14C) whereas the addition of KOX did not change the rate (Figure 14D) indicating the absence of urate oxidase in heart mitochondria.

Urate oxidase accounts for increase in oxygen consumption rate in liver.

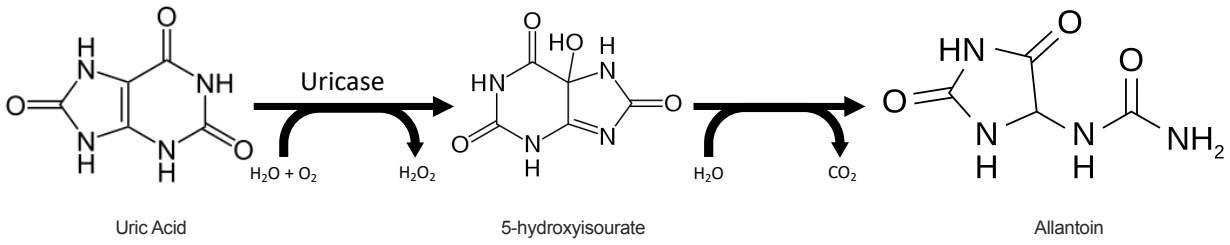

Figure 15: Representation of the oxidation of uric acid through urate oxidase (uricase).

This assay was used to determine if urate oxidase was responsible for the additional increase in oxygen consumption following the addition of uric acid in liver mitochondria (Figure 9). This assay directly compared the responses of mitochondria with and without uric acid, as well as with and without KOX to determine if KOX itself inhibited respiration. It was determined that the addition of uric acid was once again sufficient to increase the rate of oxygen consumption. Yet the

addition of uric acid with KOX showed no increase in oxygen consumption rate compared to the

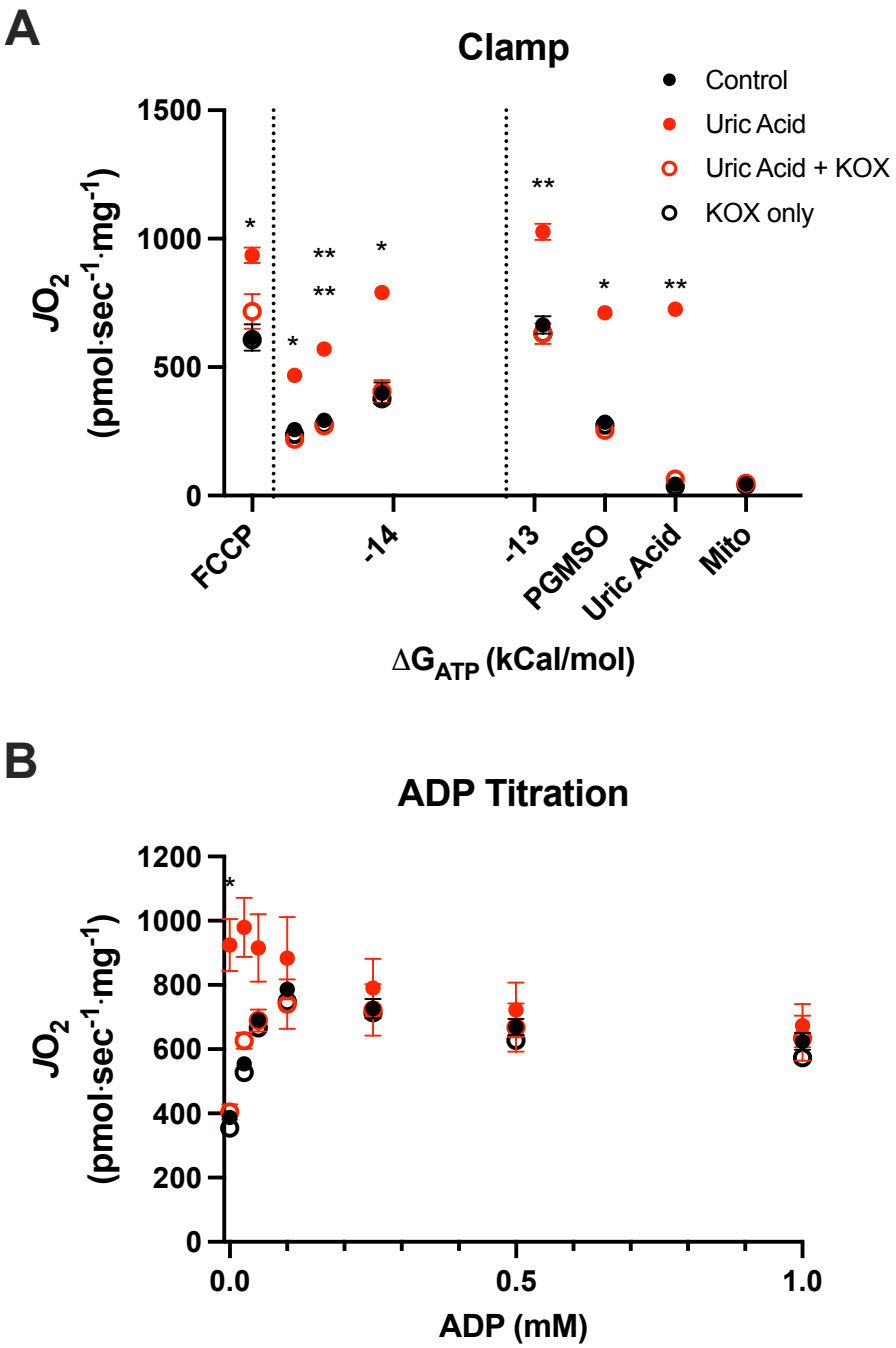

Figure 16: Validation of uricase as the source of residual oxygen consumption. (A) creatine kinase clamp assay and (B) ADP titration with isolated liver (100μg) mitochondria. All mitochondria were energized with pyruvate (5mM), glutamate (5mM), malate (2mM), succinate (5mM), and octanoyl-carnitine (0.2mM). Uric acid was given at a final concentration of 0.2mM. KOX was given at a final concentration of 9μg/mL. Data is represented as mean $\pm$ SEM, N= 3. All statistical significance denoted is as follows: 0.12 (ns), 0.033 (*), 0.002 (**), <0.001 (***).

control group (Figure 16). The addition of KOX alone also showed no change in respiration as compared to that of the control group.

DISCUSSION

A common claim up to this point in the literature is that the presence of uric acid leads to a decline in mitochondrial function[15,16,44]. To fully determine the impact uric acid has on mitochondrial bioenergetics, mitochondrial function was tested in the presence of uric acid. Overall, it was found that uric acid elicited a dose dependent increase in oxygen consumption in isolated liver mitochondria (Figure 8). This increase was found to be liver specific and was not seen in the heart. The increase in JO_2 was found to be independent of energetic state within the mitochondria, i.e., the increase was the same in both state 3 and state 4 conditions. It was also found that there was a concentration of uric acid, 0.2mM, that elicited a maximal JO_2. This increase in JO_2 was determined to remain throughout the range of steady-state ADP-stimulated respiration rates (Figure 9). However, it was found that in the liver mitochondria treated with uric acid, as the respiratory demand decreased, the difference between the treated and control respiration rates lessened, leading to an increase in slope in the uric acid treated mitochondria (Figure 9C and 9D). This suggests that the impact of uric acid on liver mitochondria differs across the range of ADP-stimulated OXPHOS demand. These findings were supported with sequential ADP additions to all mitochondria samples (Figure 10). It was found that when treated with uric acid, liver mitochondria had only about a 25% increase in JO_2 at its maximal point, whereas control mitochondria increased to about 200% at its maximal point (Figure 10A). Up to this point, all data suggested that uric acid interfered with the mitochondria's ability to respond to an ADP demand in liver mitochondria only.

Previous groups have concluded that uric acid exposure led to a rapid decrease in ATP production[29,44,67]. To determine if uric acid interfered with the OXPHOS system, the P/O assay was used. It was determined that there were no significant differences between the control and the uric acid treated group. Overall, the P/O assay indicated that there was no significant decrease in ATP production in liver mitochondria treated with uric acid (Figure 11A). While there was a significant increase in JO_2 in liver mitochondria with additional ADP additions, there was no significant differences in P/O of the controlled mitochondria (Figure 11C and 11E). There was, however, a significant increase in P/O with the addition of 200μM ADP which was maintained with the addition of 2000μM ADP. While not significant, there was a decrease in P/O between the control and uric acid treated groups, which could be explained by the increase in JO_2. This indicated that there was a drop in efficiency, i.e., requires more oxygen to produce same ATP, in liver mitochondria exposed to uric acid (Figure 11E). There was no increase in the JO_2 of the heart mitochondria exposed to uric acid in any assay. This is because urate oxidase is not expressed in the heart tissue in the mice. It is a liver specific enzyme.

A common finding in this study was the increase in JO_2 in liver mitochondria following exposure to uric acid. Previously, there has been an increase in oxidative stress associated with uric acid exposure in mitochondria[15,30,33,40,43,68]. To better determine where the excess oxygen was originating from, each complex was looked at individually (Figure 12). It was found that there was a significant increase in JO_2 in liver mitochondria exposed to uric acid (Figure 12A). This increase remained until the addition of succinate. However, since there was a significant increase in the absence of any substrates, it was determined that the likely source for the excess oxygen

consumption was a non-mitochondrial source. This was further justified by the inhibitor profile (Figure 13) in which each inhibitor failed to decrease the rate to that of the control. It is of note that the addition of malonate, a succinate oxidation inhibitor, dropped the rate, which indicated that the excess rate was linked to succinate oxidation in part (Figure 13A). To fully determine the source of oxygen consumption, the OXPHOS system was inhibited by the addition of Antimycin A (Figure 14A). While there was a slight drop in JO_2 following the inhibition of OXPHOS, there was still a significant increase when compared to that of the control. This indicated that the oxygen consumption was not linked to OXPHOS (Figure 14A). Since rodents retain urate oxidase[69], the urate oxidase inhibitor[70], KOX, was used to determine if the excess oxygen was a result of the reaction of uric acid through the oxidase as it is further metabolized to allantoin (Figure 8). It was determined that the addition of KOX was sufficient to decrease the rate of oxygen to that of the control (Figure 14B). This decrease with the addition of KOX indicated that all subsequent oxygen consumption was due to that of urate oxidase. To confirm this finding, the creatine kinase clamp assay and the ADP titration was repeated (Figure 16). These assays were redone with additional conditions, specifically KOX alone and KOX + uric acid, to determine if the presence of the inhibitor was sufficient to account for the previously unaccounted for JO_2. It was determined that with KOX present, the mitochondria treated with uric acid no longer showed an increase in JO_2 (Figure 16). This overall indicated that urate oxidate alone was responsible for the additional JO_2 seen in all experiments. When uric acid is added in addition to KOX, there is no subsequent impact on the mitochondria (Figure 16).

The presence of urate oxidase is a rodent specific phenomenon. Humans and other higher primates do not express urate oxidase. This suggests that the findings in this study were mouse specific and do not translate to a human model.

Conclusion:

It was found that uric acid does not inhibit mitochondrial bioenergetic function. Normally an increase in observed *J*O2 without a subsequent increase in *J*ATP would indicate a decrease in bioenergetic function. However, there is no observed mitochondrial decline since the increased JO_2 was found to originate from a non-mitochondrial source: urate oxidase.

This is the first data set of its kind to fully explore the mechanism behind uric acid exposure and liver mitochondria function in mice. It is known that mice retain urate oxidase, whereas humans do not, and therefore further metabolize uric acid. However, the effects of this metabolism have not been fully explored until now. This data set shows that while still present, urate oxidase must be accounted for when determining the mitochondrial implications of uric acid exposure. Relying on JO_2 alone will lead to an incomplete conclusion. While it is non-physiological, this was the most efficient way to measure the mitochondria's response to uric acid.

CHAPTER 4: Discussion

The work of this dissertation was designed to explore two main aims: 1.) To determine the effect that fructose treatment has on mitochondrial bioenergetics, and 2.) To determine the impact that uric acid exposure has on mitochondrial bioenergetics. The central hypothesis was that fructose ingestion and metabolism induces a dose-dependent and progressive fructose to AMP to uric acid induced mitochondrial bioenergetic failure, specifically that the uric acid produced following a fructose load would directly interfere with mitochondrial bioenergetic function, leading to an overall decline in the available ATP. Consequently, it was thought that all alterations to mitochondria bioenergetics following a fructose feeding could be explained by the production and presence of uric acid in the system. By understanding the role fructose plays in the development and progression of NAFLD, interventions can be explored to help alleviate the burden of disease.

Aim 1, determining the impact of fructose exposure and subsequent metabolism on liver mitochondria bioenergetics was done in several steps. The first was to determine the effects of acute fructose exposure using an acute gavage. The second was to determine the effects of chronic fructose exposure on liver mitochondria using a chronic 14-day gavage.

Aim 2, the investigation of the impact of uric acid in liver mitochondria was accomplished in several steps. The first was to determine the optimal working concentration of uric acid. This was done using a uric acid titration to determine the concentration at which uric acid induced a maximum rate of oxygen consumption. The second was to determine the direct impact of uric acid on isolated mitochondria. This was done by investigating several aspects of liver and heart

mitochondria respiration in the presence of uric acid. The third was to determine the source of added oxygen consumption rate in the presence of uric acid. This was done using specific mitochondrial and non-mitochondrial inhibitors. The final step in this aim was to confirm that urate oxidase was in fact the source of added oxygen consumption rate. This was done using potassium oxonate, KOX, to inhibit urate oxidase.

When taken together, the research explained in chapters 2 and 3 ultimately does not support the central hypothesis that fructose ingestion and metabolism induce a dose-dependent and progressive fructose to AMP to uric acid induced mitochondrial bioenergetic failure. It was found that following both a fructose and a glucose treatment, there was an increase in uric acid production in the liver. This increase in uric acid was determined to be an acute effect and not found when the mice were treated for a 14-day period. Consequently, the increase in uric acid production in the liver resulted in an increase in JO_2 in both the fructose and the glucose treated mice. It was also found that exposure to glucose alone led to a shift in mitochondrial bioenergetics, in which the presence of ATP became an inhibitory component [61] in respiration in 16-week-old mice. When challenged with an ADP demand, the 16-week-old glucose treated mice were found to be less efficient, meaning they required more oxygen to meet the same demand.

All the effects seen from the treatment with either glucose or fructose were found to be acute. Acute in this way has two separate definitions: 1.) Effects of both the glucose and the fructose gavage were only seen 15-minutes after the treatment. By the 60-minute point, there were no differences between the groups. 2.) Effects were only seen in the mice treated once. Mice that were chronically treated with either fructose or glucose did not show differences in weight, uric

acid production, or mitochondrial bioenergetic function at either the 15-minute or the 30-minute time point.

The main finding from this aim was that there was an increase in uric acid in both the glucose and the fructose treated mice. This increase was found to be shortly after gavage, within 15-minutes, and not sustained, gone by 60-minutes. The increase in uric acid was accompanied by an increase in JO_2 within 15-minutes of both fructose and glucose gavage. This correlation indicated that there was a link between the production of uric acid and a subsequent increase in JO_2 following fructose metabolism. The main conclusion from this aim was in line with the literature, there in an increase in uric acid production following a fructose challenge[15,23,30–33,71]. This increase in uric acid, both in the glucose and the fructose treated mice was accompanied by an increase in mitochondrial oxygen consumption. At this point, the study aligned with the literature in thinking that uric acid produced from fructose feeding lead to a decline in mitochondrial bioenergetic function[15,28,29,33,41,44,72,73]. To further explore the impact of uric acid on the mitochondria, Aim 2 was designed.

Aim 2 set out to fully determine the effect uric acid had on mitochondrial bioenergetics. It was confirmed in Aim 1 that fructose and glucose feeding elicited an increase in uric acid production and an increase in mitochondrial JO_2, but it was unclear as to the underlying mechanism that drove this increase.

To fully explore if uric acid was responsible for the increase in JO_2, a dose response curve was generated. From this, it was determined that there was a significant increase in JO_2 which

correlated to an increase in uric acid concentration, to a point. After 0.2mM uric acid, there was no longer an increase in JO_2 with increasing uric acid. From this point on, this was the concentration used. Using the creatine kinase assay to fully determine the response of mitochondria along the range of steady state ADP rates, it was found that after the addition of substrates and adenylates, there was a significant increase in JO_2 of liver mitochondria exposed to uric acid. At first glance, this increase appeared to be due to an increase in conductance through the electron transport system. When the mitochondria were tested with an ADP titration, the mitochondria exposed to uric acid appeared to be less efficient, meaning they required more oxygen to meet the same demand. To fully explore this, the P/O ratio was determined, and unlike previous claims, it was found that there were no significant differences in the JATP between the control and the uric acid exposed mitochondria [74]. There was, however, a significant increase in the JO_2 of the mitochondria exposed to uric acid. This indicated that there was possibly a non-mitochondrial source that accounted for the increase in JO_2. To confirm this, the complexes were study individually. It was determined that there was no single complex that contributed to the overall increase in JO_2 following uric acid exposure. When OXPHOS was inhibited, the result, no change in JO_2, confirmed that the additional oxygen consumption rate was due to a non-mitochondrial source. Considering that rodents retain the uricase enzyme within the liver, which metabolizes uric acid to allantoin at the cost of oxygen, the uricase inhibitor, KOX, was used[69,70]. The addition of KOX was sufficient to account for the additional oxygen consumption, confirming that uricase was in fact the source. It is of note that there is no uric acid effect seen in heart tissue, indicating that the increase in JO_2 following fructose and subsequently uric acid appears to be a liver specific phenomenon.

The increase in JO2 seen following the addition of uric acid was determined to be primarily due to the presence and subsequent activity of urate oxidase. However, while conserved in rodents, urate oxidase is not present in humans or higher-level primates. This ultimately means that all results in this study are not translatable to a human model. Previous studies suggests that there are mitochondrial impacts following both fructose and uric acid exposure. To fully determine the extent of the impact of both fructose and uric acid, a similar study should be done in humans.

Overall, the data in this study indicated that there was a fructose dependent increase in uric acid production, and subsequent increase in JO_2. Upon further investigation, this increased JO_2 was not attributed to the mitochondria itself. The increased JO_2 was determined to originate from the presence of urate oxidase, which metabolizes uric acid to allantoin[69,70]. Inhibition of urate oxidase was found to be sufficient to decrease the JO_2 to that of the control groups, indicating that urate oxidase was the contributing factor. Subsequently, the inhibition of urate oxidase was not found to contribute to any mitochondrial decline. Thus, it was found that fructose metabolism and ultimate uric acid production was not a significant source of mitochondrial bioenergetic failure.

Future Directions

To better understand the full mechanism behind the increase in JO_2 associated with the production of uric acid in the liver, a few questions still need to be answered:

1) *What specific mechanism is associated with the increase in flux through the purine degradation pathway resulting in an increase in production of uric acid in both fructose and glucose gavaged mice?*

While it was ultimately determined that the increase in JO_2 was due to the presence and metabolism of uric acid by urate oxidase, it was of note that there was an increase in uric acid production both the fructose and the glucose treated groups. This indicated that there was an increase in flux through the purine degradation pathway following either a fructose or a glucose gavage. Since it is thought that a shift in energy state, a drop in ATP and rise in AMP, is responsible for increased flux through the purine degradation pathway, a study can be designed to determine if a gavage of either fructose or glucose leads to the same shift in energy balance. At each timepoint, a measure of the total adenylate pool will help to determine the concentration of each. To this, there could also be time points added to mark when the production of uric acid is first detected in the liver and when it is first detected in the blood.

2) *Is the presence of ATP acting as an inhibitory regulator of OXPHOS in liver mitochondria following a glucose gavage?*

A second interesting aspect of the gavaged treatments was that in the 16-week-old mice, there was a drop in JO_2 of the glucose treated mice with the increase in concentration of ATP. This was an indication that the presence of ATP was itself inhibitory in mice exposed to a bolus of glucose[61]. One potential explanation would be that this experiment was limited by the substrate condition, succinate only, and this could be repeated in the presence of various substrate

combinations. If this is a persistent finding, it would be beneficial to expand this assay to include several other tissues, i.e., heart, skeletal muscle, and fat. If this finding does not surface in additional tissues, it could indicate that the liver tissue is intrinsically set up for a low ATP environment. Since the liver tissue is not a highly ATP productive tissue to begin with, the regulation of ATP production by the presence of ATP would be a logical one.

3) *With the presence of succinate alone, is the failure to reach a higher JO_2 following FCCP addition due to substrate availability?*

A third finding in this project was the inability to recover a state 3 respiration rate following FCCP addition. In the gavaged mice, there was no increase of JO_2 past that of the succinate supported rate at any of the measured timepoints. This, once again, could be due to the use of succinate alone as a substrate source. The addition of FCCP could potentially crash the membrane potential and since succinate is the only substrate, there is no additional proton pumping, thus no recovery of potential[61]. To determine if this is the underlying cause, membrane potential assays can be ran using tetramethylrhodamine, methyl ester (TMRM). TMRM is a fluorescent dye used to measure the membrane potential between the interior and exterior membranes in the mitochondria. By measuring both the JO_2 and the membrane potential together, it can be determined if the drop in JO_2 is in fact from a depolarization event.

The final, and possibly most important question left to be answered in this study is:

4) *In humans, is there an impact of uric acid on mitochondrial bioenergetics?*

Previous data suggests that HepG2 cells exposed to uric acid exhibit and immediate and sustained drop in mitochondrial membrane potential. While it was determined that there was no impact of fructose or uric acid on mitochondria isolated from mouse liver, it is unclear if the same is true for liver mitochondria from a human.

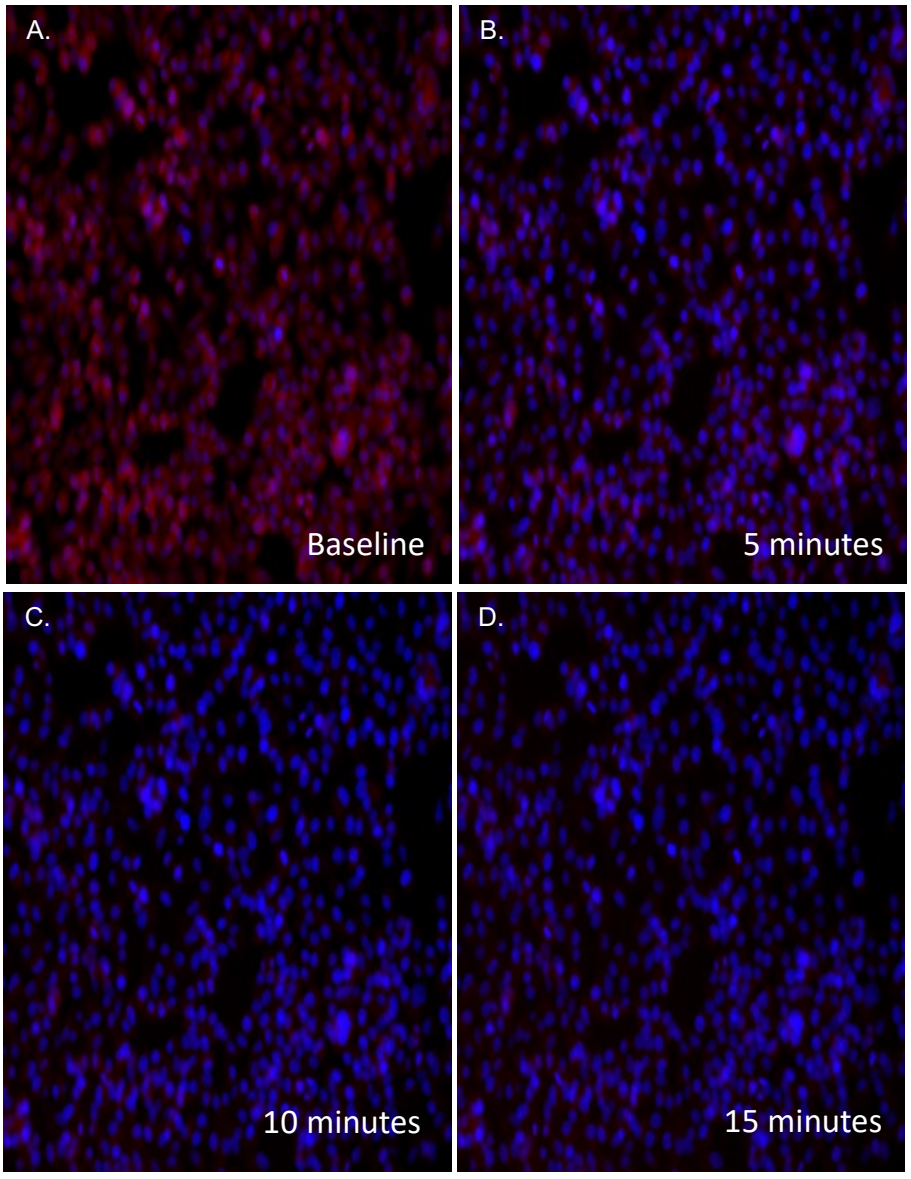

Figure 17: Mitochondrial membrane potential measurement of HepG2 cells following uric acid exposure. Nuclei stained with DAPI (blue) and membrane potential measured with TMRM (red). Uric acid (0.1mM) was added a single time and fluorescence was monitored following exposure.

to fully determine if the results seen in this study are not translatable to humans, a simple study can be done in which HepG2 cells, a human cell line, and Hepa 1-6 cells, an equivalent mouse cell line, can be used. These cells can be grown then exposed to uric acid and the membrane potentials can be determined as before. If there are differences between the mouse and the human finding, there is sufficient evidence to justify the findings in this study as mouse specific. If there is a drop in membrane potential in the human cells and not the mouse cells, there should be subsequent experiments to determine the impact of uric acid on human liver mitochondria.

REFERENCES:

1. Softic S, Cohen DE, Kahn • C Ronald, Kahn CR. Role of Dietary Fructose and Hepatic De Novo Lipogenesis in Fatty Liver Disease. *Digestive Diseases and Sciences*. 2016;61:1282-1293. doi:10.1007/s10620-016-4054-0
2. Ford ES, Giles WH, Mokdad AH. *Increasing Prevalence of the Metabolic Syndrome Among U.S. Adults*.; 2004.
3. Gotto Jr AM, Blackburn GL, Dailey III GE, et al. *The Metabolic Syndrome: A Call to Action Correspondence and Requests for Reprints To*. Vol 17. Lippincott Williams & Wilkins; 2006. www.eatlas.idf.org
4. Perumpail BJ, Khan MA, Yoo ER, Cholankeril G, Kim D, Ahmed A. Clinical epidemiology and disease burden of nonalcoholic fatty liver disease. *World Journal of Gastroenterology*. 2017;23(47):8263-8276. doi:10.3748/wjg.v23.i47.8263
5. Paschos P, Paletas K. Non alcoholic fatty liver disease and metabolic syndrome. *HIPPOKRATIA*. 2009;13(1):9-19.
6. Friedman SL, Neuschwander-Tetri BA, Rinella M, Sanyal AJ. Mechanisms of NAFLD development and therapeutic strategies. *Nature Medicine*. doi:10.1038/s41591-018-0104-9
7. Donnelly KL, Smith CI, Schwarzenberg SJ, Jessurun J, Boldt MD, Parks EJ. Sources of fatty acids stored in liver and secreted via lipoproteins in patients with nonalcoholic fatty liver disease. *The Journal of Clinical Investigation*. 2005;115. doi:10.1172/JCI200523621
8. Fabbrini E, Dehaseth D, Deivanayagam S, Mohammed BS, Vitola BE, Klein S. Alterations in fatty acid kinetics in obese adolescents with increased intrahepatic triglyceride content. *Obesity*. 2009;17(1):25-29. doi:10.1038/oby.2008.494
9. Cali AMG, Zern TL, Taksali SE, et al. Intrahepatic Fat Accumulation and Alterations in Lipoprotein Composition in Obese Adolescents A perfect proatherogenic state. *Diabetes Care*. 2007;30:3093-3098. doi:10.2337/dc07
10. Maurizio Cassadera, Roberto Gambinoa, Giovanni Mussoa, et al. Postprandial Triglyceride-Rich LipoproteinMetabolism and Insulin Sensitivity in Nonalcoholic Steatohepatitis Patients. Published online October 2001:1117-1124.
11. Diraison F, Moulin PH, Beylot M. Contribution of hepatic de novo lipogenesis and reesterification of plasma non esterified fatty acids to plasma triglyceride synthesis during non-alcoholic fatty liver disease. *Diabetes and Metabolism*. 2003;29(5):478-485. doi:10.1016/S1262-3636(07)70061-7
12. Vos MB, Lavine JE. Dietary fructose in nonalcoholic fatty liver disease. *Hepatology*. 2013;57(6):2525-2531. doi:10.1002/hep.26299
13. Andres-Hernando A, Orlicky DJ, Kuwabara M, et al. Deletion of Fructokinase in the Liver or in the Intestine Reveals Differential Effects on Sugar-Induced Metabolic Dysfunction. *Cell Metabolism*. 2020;32(1):117-127.e3. doi:10.1016/j.cmet.2020.05.012
14. Cox CL, Stanhope KL, Schwarz JM, et al. Consumption of fructose-sweetened beverages for 10 weeks reduces net fat oxidation and energy expenditure in overweight/obese men and women. *European Journal of Clinical Nutrition*. 2012;66(2):201-208. doi:10.1038/ejcn.2011.159
15. Nakagawa T, Hu H, Zharikov S, et al. A causal role for uric acid in fructose-induced metabolic syndrome. *American Journal of Physiology - Renal Physiology*. 2006;290(3):F625-F631. doi:10.1152/ajprenal.00140.2005

16. Cox CL, Stanhope KL, Schwarz JM, et al. Consumption of fructose- but not glucose-sweetened beverages for 10 weeks increases circulating concentrations of uric acid, retinol binding protein-4, and gamma-glutamyl transferase activity in overweight/obese humans. *Nutrition and Metabolism*. 2012;9(1):1. doi:10.1186/1743-7075-9-68
17. Stanhope KL, Bremer AA, Medici V, et al. Consumption of fructose and high fructose corn syrup increase postprandial triglycerides, LDL-cholesterol, and apolipoprotein-B in young men and women. *Journal of Clinical Endocrinology and Metabolism*. 2011;96(10):1596-1605. doi:10.1210/jc.2011-1251
18. Tappy L, Lê KA. Metabolic Effects of Fructose and the Worldwide Increase in Obesity. *Physiological Reviews*. 2010;90(1):23-46. doi:10.1152/physrev.00019.2009
19. Herman MA, Samuel VT. The Sweet Path to Metabolic Demise: Fructose and Lipid Synthesis. *Trends in endocrinology and metabolism: TEM*. 2016;27(10):719-730. doi:10.1016/j.tem.2016.06.005
20. Bray GA, Nielsen SJ, Popkin BM. Consumption of high-fructose corn syrup in beverages may play a role in the epidemic of obesity. *The American Journal of Clinical Nutrition*. 2004;79(4):537-543. doi:10.1093/ajcn/79.4.537
21. Elliott SS, Keim NL, Stern JS, Teff K, Havel PJ. Fructose, weight gain, and the insulin resistance syndrome 1-3. *American Journal of Clinical Nutrition*. 2002;76:911-922. https://academic.oup.com/ajcn/article/76/5/911/4689540
22. Schwarz JM, Schutz Y, Froidevaux F, et al. Thermogenesis in men and women induced by fructose vs glucose added to a meal. *American Journal of Clinical Nutrition*. 1989;49(4):667-674. doi:10.1093/ajcn/49.4.667
23. Mayes PA. Intermediary metabolism of fructose. *The American Journal of Clinical Nutrition*. 1993;58(5):754S-765S. doi:10.1093/ajcn/58.5.754S
24. Herman MA, Samuel VT. The Sweet Path to Metabolic Demise: Fructose and Lipid Synthesis. *Trends in endocrinology and metabolism: TEM*. 2016;27(10):719-730. doi:10.1016/j.tem.2016.06.005
25. Bode JCh, Zelder O, Rumpelt HJ, Wittkampy U. Depletion of Liver Adenosine Phosphates and Metabolic Effects of Intravenous Infusion of Fructose or Sorbitol in Man and in the Rat ، **. *European Journal of Clinical Investigation*. 1973;3(5):436-441. doi:10.1111/j.1365-2362.1973.tb02211.x
26. Hultman E, von Nilsson LH, Sahlin K. Adenine nucleotide content of human liver normal values and fructose-induced depletion. *Scandinavian Journal of Clinical and Laboratory Investigation*. 1975;35(3):245-251. doi:10.1080/00365517509095736
27. Oberhaensli RD, Galloway GJ, Taylor DJ, Bore PJ, Radda GK. Assessment of human liver metabolism by phosphorus-31 magnetic resonance spectroscopy. *British Journal of Radiology*. 1986;59(703):695-699. doi:10.1259/0007-1285-59-703-695
28. King C, Lanaspa MA, Jensen T, et al. Uric Acid as a Cause of the Metabolic Syndrome. *Contrib Nephrol Basel, Karger*. 2018;192:88-102. doi:10.1159/000484283
29. Softic S, Meyer JG, Wang GX, et al. Dietary Sugars Alter Hepatic Fatty Acid Oxidation via Transcriptional and Post-translational Modifications of Mitochondrial Proteins. *Cell Metabolism*. 2019;30(4):735-753.e4. doi:10.1016/j.cmet.2019.09.003
30. Heuckenkamp PU, Zöllner N. Fructose-Induced Hyperuricæmia. *The Lancet*. 1971;297(7703):808-809. doi:10.1016/S0140-6736(71)91259-1
31. Kogut ED. *Fructose-Induced Hyperuricemia: Observations in Normal Children and in Patients with Hereditary Fructose Intolerance and Galactosemia*.

32. Shi Y, Williamson G. Quercetin lowers plasma uric acid in pre-hyperuricaemic males: a randomised, double-blinded, placebo-controlled, cross-over trial. *British Journal of Nutrition*. 2016;115(05):800-806. doi:10.1017/s0007114515005310
33. Caliceti C, Calabria D, Roda A, Cicero A. Fructose Intake, Serum Uric Acid, and Cardiometabolic Disorders: A Critical Review. *Nutrients*. 2017;9(4):395. doi:10.3390/nu9040395
34. Lanaspa MA, Cicerchi C, Garcia G, et al. Counteracting Roles of AMP Deaminase and AMP Kinase in the Development of Fatty Liver. *PLoS ONE*. 2012;7(11). doi:10.1371/journal.pone.0048801
35. Johnson RJ, Sautin YY, Oliver WJ, et al. Lessons from comparative physiology: could uric acid represent a physiologic alarm signal gone awry in western society? *Journal of Comparative Physiology B*. 2009;179(1):67-76. doi:10.1007/s00360-008-0291-7
36. Oppelt SA, Sennott EM, Tolan DR. Aldolase-B knockout in mice phenocopies hereditary fructose intolerance in humans. *Molecular Genetics and Metabolism*. 2015;114(3):445-450. doi:10.1016/j.ymgme.2015.01.001
37. Lanaspa MA, Andres-Hernando A, Orlicky DJ, et al. Ketohexokinase C blockade ameliorates fructose-induced metabolic dysfunction in fructose-sensitive mice. *Journal of Clinical Investigation*. 2018;128(6):2226-2238. doi:10.1172/JCI94427
38. Lameire N, Mussche M, Baele G, Kint J, Ringoir S. Hereditary fructose intolerance: A difficult diagnosis in the adult. *The American Journal of Medicine*. 1978;65(3):416-423. doi:10.1016/0002-9343(78)90767-2
39. Kono H, Rusyn I, Bradford BU, Connor HD, Mason RP, Thurman RG. Allopurinol prevents early alcohol-induced liver injury in rats. *The Journal of pharmacology and experimental therapeutics*. 2000;293(1):296-303.
40. Lanaspa MA, Sanchez-Lozada LG, Choi YJ, et al. Uric acid induces hepatic steatosis by generation of mitochondrial oxidative stress: Potential role in fructose-dependent and -independent fatty liver. *Journal of Biological Chemistry*. 2012;287(48):40732-40744. doi:10.1074/jbc.M112.399899
41. Johnson RJ, Nakagawa T, Sanchez-Lozada LG, et al. Sugar, uric acid, and the etiology of diabetes and obesity. *Diabetes*. 2013;62(10):3307-3315. doi:10.2337/db12-1814
42. Jensen T, Abdelmalek MF, Sullivan S, et al. Fructose and Sugar: A Major Mediator of Nonalcoholic Fatty Liver Disease HHS Public Access. *J Hepatol*. 2018;68(5):1063-1075. doi:10.1016/j.jhep.2018.01.019
43. Beysen C, McGahan JP, Nakano T, et al. Consuming fructose-sweetened, not glucose-sweetened, beverages increases visceral adiposity and lipids and decreases insulin sensitivity in overweight/obese humans. *Journal of Clinical Investigation*. 2009;119(5):1322-1334. doi:10.1172/jci37385
44. Yang Y, Zhou Y, Cheng S, Sun JL, Yao H, Ma L. Effect of uric acid on mitochondrial function and oxidative stress in hepatocytes. *Genetics and Molecular Research*. 2016;15(2). doi:10.4238/gmr.15028644
45. Prager GN, Ontko JA. Direct effects of fructose metabolism on fatty acid oxidation in a recombined rat liver mitochondria-high speed supernatant system. *Biochimica et Biophysica Acta (BBA)/Lipids and Lipid Metabolism*. 1976;424(3):386-395. doi:10.1016/0005-2760(76)90028-X

46. van den Berghe G, Bronfman M, Vanneste R, Hers HG. The mechanism of adenosine triphosphate depletion in the liver after a load of fructose. A kinetic study of liver adenylate deaminase. *Biochemical Journal*. 2015;162(3):601-609. doi:10.1042/bj1620601
47. García-Berumen CI, Ortiz-Avila O, Vargas-Vargas MA, et al. The severity of rat liver injury by fructose and high fat depends on the degree of respiratory dysfunction and oxidative stress induced in mitochondria. doi:10.1186/s12944-019-1024-5
48. MIRANDA CA, SCHÖNHOLZER TE, KLÖPPEL E, et al. Repercussions of low fructose-drinking water in male rats. *Anais da Academia Brasileira de Ciências*. 2019;91(1). doi:10.1590/0001-3765201920170705
49. García-Arroyo FE, Monroy-Sánchez F, Muñoz-Jiménez I, et al. Allopurinol prevents the lipogenic response induced by an acute oral fructose challenge in short-term fructose fed rats. *Biomolecules*. 2019;9(10):1-14. doi:10.3390/biom9100601
50. Fossati P, Prencipe L, Berti G. Use of 3,5-dichloro-2-hydroxybenzenesulfonic acid/4-aminophenazone chromogenic system in direct enzymic assay of uric acid in serum and urine. *Clinical Chemistry*. 1980;26(2):227-231.
51. Ames BN, Cathcart R, Schwiers E, Hochsteint P. Uric acid provides an antioxidant defense in humans against oxidant-and radical-caused aging and cancer: A hypothesis (lipid peroxidation/ascorbic acid/primate evolution/erythrocyte aging). *Proc NatL Acad Sci USA*. 1981;78(11):6858-6862. http://www.pnas.org/content/pnas/78/11/6858.full.pdf
52. Frezza C, Cipolat S, Scorrano L. Organelle isolation: functional mitochondria from mouse liver, muscle and cultured filroblasts. Published online 2007. doi:10.1038/nprot.2006.478
53. Perry CGR, Kane DA, Lanza IR, Darrell Neufer P. Methods for Assessing Mitochondrial Function in Diabetes. *Diabetes*. 2013;62:1041-1053. doi:10.2337/db12-1219
54. Lark DS, Torres MJ, Lin CT, Ryan TE, Anderson EJ, Darrell Neufer P. Direct real-time quantification of mitochondrial oxidative phosphorylationefficiency in permeabilized skeletal muscle myofibers. *Am J Physiol Cell Physiol*. 2016;311:239-245. doi:10.1152/ajpcell.00124.2016.-Oxidative
55. Glancy B, Willis WT, Chess DJ, Balaban RS. Effect of calcium on the oxidative phosphorylation cascade in skeletal muscle mitochondria. *Biochemistry*. 2013;52(16):2793-2809. doi:10.1021/bi3015983
56. Messer JI, Jackman MR, Willis WT, Willis WT. Pyruvate and citric acid cycle carbon requirements in isolated skeletal muscle mitochondria. *Am J Physiol Cell Physiol*. 2004;286:565-572. doi:10.1152/ajpcell.00146.2003.-Carbohydrate
57. Fisher-Wellman KH, Davidson MT, Narowski TM, Lin C te, Koves TR, Muoio DM. Mitochondrial Diagnostics: A Multiplexed Assay Platform for Comprehensive Assessment of Mitochondrial Energy Fluxes. *Cell Reports*. 2018;24(13):3593-3606.e10. doi:10.1016/j.celrep.2018.08.091
58. Golding E, Teague W, Dobson G. Adjustment of K' to varying pH and pMg for the creatine kinase, adenylate kinase and ATP hydrolysis equilibria permitting quantitative bioenergetic assessment - PubMed. *The Journal of Experimental Biology*. 1995;198(8):1775-1782. Accessed September 12, 2021. https://pubmed.ncbi.nlm.nih.gov/7636446/
59. Buddo KA, Goldberg, Emma J.McLaughlin KL, Fernandez RF, et al. Correction: Tissue-specific characterization of mitochondrial branched-chain keto acid oxidation using a multiplexed assay platform (Biochemical Journal (2019) 476 (1521–1537) DOI:

10.1042/BCJ20190182). *Biochemical Journal*. 2019;476(17):2519. doi:10.1042/BCJ-2019-0182_COR
60. Torres MJ, Kew KA, Ryan TE, et al. 17β-Estradiol Directly Lowers Mitochondrial Membrane Microviscosity and Improves Bioenergetic Function in Skeletal Muscle. *Cell Metabolism*. 2018;27(1):167-179.e7. doi:10.1016/j.cmet.2017.10.003
61. Mclaughlin KL, Hagen JT, Coalson HS, et al. Novel approach to quantify mitochondrial content and intrinsic bioenergetic efficiency across organs. Published online 2020. doi:10.1038/s41598-020-74718-1
62. Fisher-wellman KH, Fisher-wellman KH, Williams A, Stevens R, Olson D. Cell Reports Respiratory phenomics across multiple models of protein hyperacylation in cardiac mitochondria reveals a marginal impact on bioenergetics.
63. Vyssokikh MY, Holtze S, Averina OA, et al. Mild depolarization of the inner mitochondrial membrane is a crucial component of an anti-aging program. *Proceedings of the National Academy of Sciences of the United States of America*. 2020;117(12):6491-6501. doi:10.1073/pnas.1916414117
64. Malik VS, Pan A, Willett WC, et al. Potential role of sugar (fructose) in the epidemic of hypertension, obesity and the metabolic syndrome, diabetes, kidney disease, and cardiovascular disease. *The American Journal of Clinical Nutrition*. 2013;86(3):1-15. doi:10.1016/j.ctcp.2012.12.002
65. Ryan TE, Schmidt CA, Tarpey MD, et al. PFKFB3-mediated glycolysis rescues myopathic outcomes in the ischemic limb. Published online 2020. doi:10.1172/jci.insight.139628
66. Ryan TE, Schmidt CA, Alleman RJ, et al. Mitochondrial therapy improves limb perfusion and myopathy following hindlimb ischemia - ClinicalKey. *Journal of Molecular and Cellular Cardiology*. Published online 2016:191-196. Accessed September 12, 2021. https://www.clinicalkey.com/#!/content/playContent/1-s2.0-S002228281630147X?scrollTo=%23hl0000207
67. Brault JJ, Pizzimenti NM, Dentel JN, Wiseman RW. Selective inhibition of ATPase activity during contraction alters the activation of p38 MAP kinase isoforms in skeletal muscle. *Journal of Cellular Biochemistry*. 2013;114(6):1445-1455. doi:10.1002/jcb.24486
68. Jensen T, Abdelmalek MF, Sullivan S, et al. Fructose and sugar: A major mediator of non-alcoholic fatty liver disease. *Journal of Hepatology*. 2018;68(5):1063-1075. doi:10.1016/j.jhep.2018.01.019
69. Mikami T, Sorimachi M. Uric acid contributes greatly to hepatic antioxidant capacity besides protein. *Physiological Research*. 2017;66(6):1001-1007.
70. Tang DH, Ye YS, Wang CY, Li ZL, Zheng H, Ma KL. Potassium oxonate induces acute hyperuricemia in the tree shrew (Tupaia belangeri chinensis). *Experimental Animals*. 2017;66(3):209-216. doi:10.1538/expanim.16-0096
71. Sarah A. Hannou, Danielle E. Haslam, Nicola M. McKeown, Mark A. Herman. Fructose Metabolism and Metabolic Disease. *The Journal of Clinical Investigation*. 2018;128(2):545-555. doi:10.1172/JCI96702
72. Softic S, Cohen DE, Kahn CR. Role of Dietary Fructose and Hepatic De Novo Lipogenesis in Fatty Liver Disease. *Digestive Diseases and Sciences*. 2016;61(5):1282-1293. doi:10.1007/s10620-016-4054-0
73. So A, Thorens B. Uric acid transport and disease. *Journal of Clinical Investigation*. 2010;120(6):1791-1799. doi:10.1172/JCI42344

74. Marciani L, Stephenson MC, Hunter K, et al. Investigating the effects of an oral fructose challenge on hepatic ATP reserves in healthy volunteers: A 31P MRS study. *Clinical Nutrition*. 2015;35(3):645-649. doi:10.1016/j.clnu.2015.04.001

APPENDIX A: IACUC Approval Letters

ECU

Animal Care and Use Committee
212 Ed Warren Life Sciences Building | East Carolina University | Greenville, NC 27834-4354
252-744-2436 office | 252-744-2355 fax

October 25, 2018

Darrell Neufer, Ph.D.
Department of Physiology/ECDOI
ECHI 4th floor
East Carolina University

Dear Dr. Neufer:

Your Animal Use Protocol entitled, "Breeding of Mice for Mitochondrial Bioenergetics and Metabolic Disease Studies" (AUP #Q285c) was reviewed by this institution's Animal Care and Use Committee on October 25, 2018. The following action was taken by the Committee:

"Approved as submitted"

Please contact Aaron Hinkle at 744-2997 prior to hazard use

A copy is enclosed for your laboratory files. Please be reminded that all animal procedures must be conducted as described in the approved Animal Use Protocol. Modifications of these procedures cannot be performed without prior approval of the ACUC. The Animal Welfare Act and Public Health Service Guidelines require the ACUC to suspend activities not in accordance with approved procedures and report such activities to the responsible University Official (Vice Chancellor for Health Sciences or Vice Chancellor for Academic Affairs) and appropriate federal Agencies. **Please ensure that all personnel associated with this protocol have access to this approved copy of the AUP and are familiar with its contents.**

Sincerely yours,

Susan McRae, Ph.D.
Chair, Animal Care and Use Committee

SM/jd

Enclosure